LAPPEENRANTA
UNIVERSITY OF TECHNOLOGY

Faculty of Technology
Department of Technical Physics and Mathematics

Dominique Habimana

Statistical Optimum Design of Heat Exchangers

The topic of this Master's thesis was approved by the departmental council of the Department of Technical Physics and Mathematics on 12 December 2008.

The examiners of the thesis were Professor Heikki Haario and PhD Tuomo Kauranne.
The thesis was supervised by Professor Heikki Haario.

Lappeenranta, January 30, 2009

Dominique Habimana
Punkkerikatu 7 A 12
53850 Lappeenranta
+358 400 166474
Dominique.Habimana@lut.fi

ABSTRACT

Lappeenranta University of Technology
Department of Technical Physics and Mathematics

Author: Dominique Habimana

Subject: **Statistical Optimum Design of Heat Exchangers**

Master's thesis.

Year: 2009

Lappeenranta University of Technology. 72 pages, 15 figures, 7 tables and 5 appendices.

Supervisor: Professor Heikki Haario
PhD Tuomo Kauranne

Advisor: M.Sc Kalle Riihimäki

Keywords: Heat Exchanger Network, Genetic Algorithm, MCMC.

The optimal design of a heat exchanger system is based on given model parameters together with given standard ranges for machine design variables. The goals set for minimizing the Life Cycle Cost (LCC) function which represents the price of the saved energy, for maximizing the momentary heat recovery output with given constraints satisfied and taking into account the uncertainty in the models were successfully done.

Nondominated Sorting Genetic Algorithm II (NSGA-II) for the design optimization of a system is presented and implemented in Matlab environment. Markov Chain Monte Carlo (MCMC) methods are also used to take into account the uncertainty in the models. Results show that the price of saved energy can be optimized. A wet heat exchanger is found to be more efficient and beneficial than a dry heat exchanger even though its construction is expensive (160 EUR/m^2) compared to the construction of a dry heat exchanger (50 EUR/m^2). It has been found that the longer lifetime weights higher CAPEX and lower OPEX and vice versa, and the effect of the uncertainty in the models has been identified in a simplified case of minimizing the area of a dry heat exchanger.

PREFACE

This Master's thesis is based on research work carried out at the Department of Technical Physics and Mathematics, Lappeenranta University of Technology, and funded by the TM Systems Finland Oy, as a part of the MASI technology program.

I wish to express my deepest gratitude to my supervisor Professor Heikki Haario, who gave me the chance to work on this project. I am grateful to him for all of his invaluable support during my work with him, and I would like to thank him very much for his supervision and guidance through the work of this thesis.

I would like to express my gratitude to examiner Ph.D. Tuomo Kauranne for reviewing this thesis and his valuable comments and his encouragement in scientific research activities point of view. I would also like to thank very much Kalle Riihimäki for his intensive explanations of heat exchanger processes during this project work.

I would like to thank Professor Verdiana Grace Masanja and Ph.D. Matti Heiliö for their effort in establishing the cooperation between Lappeeanranta University of Technology and my home university Kigali Institute of Science and Technology (KIST) which allowed me to pursue my studies in Finland. Special thanks go to KIST for their financial support to my family during my studies.

Many thanks go to Taavi Aalto and Saku Kukkonen for their fruitful cooperation through the whole work. Many thanks go to all of my colleagues at the Department of Technical Physics and Mathematics. Special thanks go to Piotr Ptak, Karita Riekko and Kauppi Helkky for their support and guidance during my first days in Finland. Additionally, my special thanks are to my colleagues Jere Heikkinen, Matylda Jablonska and Tapio Leppälampi.

No words are able to express how grateful I am to my wife Nyiragwiza Lucie for all her love and care and her continuous encouragement, without which this work would not have been achievable. I would like also to mention my son, Kuzwa Manzi Davin Praise, with him this work was difficult to accomplish, but without him there would be no meaning in life.

UGUSHIMIRA

Iki gitabo gisoza amasomo y'impamyabushobozi y'ikirenga gikubiyemo ubushakashatsi bwakorewe mu ishami ry'Imibare n'Ubugenge, muri Kaminuza y'Ikoranabuhanga ya Lappeenranta, kandi buterwa inkunga n'Ikigo Cy'igihugu cya Finilande gishinzwe ubushakashatsi n'ikoranabuhanga.

Nejejwe no gushimira cyane umugenzuzi wanjye Mwarimu Heikki Haario, wampaye amahirwe yo gukora kuri uyu mushinga. Ndamushimira cyane ku kwitanga kwe kutagereranywa, ubugenzuzi n'inama ze nziza mu gihe iki gitabo cyandikwaga.

Ndashimira cyane Umuhanga Tuomo Kauranne wasuzumye kandi agakosora iki gitabo ku bw'inama ze nziza zitagira akagero. Ndongera gushimira cyane kandi Kalle Riihimäki witanze mu kunsobanurira uko imashini zitanga ubushyuhe cyangwa ubukonje mu nganda zikora muri uyu mushinga.

Ndashimira cyane kandi Mwalimu Verdiana Grace Masanja n'Umuhanga Matti Heiliö ku bw'umuhate n'imbaraga bakoresheje mu gushaka umubano hagati ya Kaminuza y'ikoranabuhanga ya Lappeenranta n'Ishuli rikuru ry'ubushakashatsi n'ikoranabuhanga mu Rwanda, byatumye mbasha gukomeza amashuli yanjye mu gihugu cya Finilande. Nshimiye by'umwihariko ishuli rikuru ry'ubushakashatsi n'ikoranabuhanga rya Kigali ryanteye inkugu umuryango wanjye mu gihe nigaga.

Nshimiye cyane Taavi Aalto na Saku Kukkonen bambaye hafi muri aka kazi. Nshimiye nanone abanyeshuli bagenzi banjye bo mu ishami ry'imibare n'ubugenge. Nshimiye by'umwihariko Piotr Ptak, Karita Riekko na Kauppi Helkky ku bw'ubufasha bwabo n'inama zabo mu minsi yanjye ya mbere ngeze Finilande. Nshimiye kandi by'umwihariko inshuti zanjye Jere Heikkinen,Matylda Jablonska na Tapio Leppälampi.

Sinabona amagambo nshimiramo umufasha wanjye Nyiragwiza Lucie ku bw'urukundo rwe rutagereranwa, kumba hafi no kuntera imbaraga bya buri munsi, ibi byose iyo bitahaba iki gikorwa nticyari kugera ku musozo. Ndongeraho kandi umuhungu wanjye, Kuzwa Manzi Davin Praise, kuba kure ye byatumye iki gikorwa kigorana, ariko kandi kutamugira ubuzima ntacyo bwari kuba buvuze kuri jye.

Contents

1 Introduction **8**

2 Problem Description **10**

3 Structure and Operating Principals of Dryer Section Heat Recovery **11**

3.1 Thermodynamics of Dryer Section Heat Recovery 15

3.2 Empirical Correlations for Convection Coefficient 16

4 Paper Machine Heat Exchangers **17**

4.1 Heat Exchanger Analysis 18

4.1.1 The Parallel-Flow Heat Exchanger 19

4.1.2 The Counterflow Heat Exchanger 21

4.1.3 Dry and Wet Heat Exchanger Models 22

4.2 Calculation of Pressure Drop 24

5 Optimization Models and Techniques **26**

5.1 Optimization Models 26

5.2 Life Cycle Cost (LCC) 27

5.3 Combination of Simulation and Optimization 32

5.4 Genetic Algorithm (GA) 34

5.4.1 Multi-Objective Genetic Algorithm (MOGA) 35

5.4.2 Elitist Nondominated Sorting Genetic Algorithm II (NSGA-II) . . 36

6 Markov Chain Monte Carlo Methods in Optimizing a Heat Exchanger Network 41

6.1 Bayesian Inference in Parameter Estimation 41

6.1.1 Bayes' Rule 42

6.1.2 Prior Distributions 44

6.1.3 Likelihood in Parameter Estimation 44

6.1.4 Point Estimates 45

6.2 Monte Carlo Methods 47

6.3 Markov Chain Monte Carlo Methods 47

6.3.1 Metropolis-Hastings Algorithm 48

6.3.2 MCMC Sampling and how the Chain is used Inside the Optimizer 49

7 Implementation Methodology of the Case Study 52

7.1 Structure of the Heat Recovery Units used in the Case Study 52

7.1.1 Dry Heat Recovery Unit 52

7.1.2 Wet Heat Recovery Unit 53

7.2 Model Calculation and Control Variable Selection 53

8 Results 58

8.1 Optimization Results 58

8.1.1 Results from the Dry Heat Exchanger Sub-process 60

8.1.2 Results from the Whole System 62

8.2 Results from the MCMC Methods for the Dry Heat Exchanger Sub-process 64

8.3 Discussion and Future Work 67

9 Conclusions **68**

References **70**

Appendices **73**

VOCABULARY

CAPEX	Capital Expenditures
CI	Confidence Interval
GA	Genetic Algorithm
LB	Lower Bound
LCC	Life Cycle Cost
MC	Monte Carlo
MCMC	Markov Chain Monte Carlo
MAP	Maximum A Posteriori
ML	Maximum Likelihood
MLE	Maximum Likelihood Estimate
MOGA	Multi-objective Genetic algorithm
NSGA	Nondominated Sorting Genetic Algorithm
NTU	Number of Transfer Units
OPEX	Operating Expenditures
PDF	Probability Density Function
PHR	Plate Heat Recovery
STHE	Shell-and-Tube Heat Exchanger
UB	Upper Bound

NOTATIONS

General

A	area	[m^2]
$a^{'}$	present value factor	[-]
$a^{''}$	escalation term	[%/a]
C	constant	[-]
C	covariance	[-]
c_p	specific heat capacity	[kJ/kgK]
d	slot size	[m]
D	hydaulic diameter	[m]
e	energy price	[EUR/kWh]
E	energy	[kWh]
F	correction factor	[-]
f	friction factor	[-]
$f(X\|\theta)$	model with known X and unknown parameters θ	[-]
H	height	[m]
h	mass specific enthalpy	[kJ/kg]
I	investment	[EUR]
K	loss coefficient	[-]
K	annual maintenance costs of the system	[EUR/a]
k	thermal conductivity of the fluid	[W/mK]
L	length	[m]
l	latent heat	[kJ/kg]
ln	natural logarithm	[-]
N	number of slots	[-]
Nu	Nusselt number	[-]
P	pressure	[Pa]
p	probability	[-]
$p(\theta\|Y)$	joint probability distribution of θ and Y	[-]
$p(Y\|\theta)$	likelihood	[-]
p_ϵ	PDF of error ϵ	[-]
Pr	Prandtl number	[-]
r	nominal interest rate	[%/a]
Re	Reynolds number	[-]

S	thickness	[m]
SS_θ	sum of squares with parameters θ	[-]
T	temperature	[^{o}C]
t	life span of the project	[a]
q_m	mass flow rate	[kg/s]
$q(.\|\theta)$	proposal distribution at point θ	[-]
Y	Measurements	[-]
V	volumetric flow rate	[m^3/s]
U	overall heat transfer coefficient	[W/m^{2}K]
w	fluid velocity	[m/s]
x	absolute humidity of air	[gH_2O/kg]
X	design matrix	[-]
W	width	[m]

Greek letters

α	heat transfer coefficient	[W/m^{2}K]
Δ	difference	[-]
ϵ	measurement error	[-]
Φ	heat transfer energy	[kW]
Φ''	heat flux	[W/m^2]
μ	dynamic viscosity of the fluid	[kg/s m]
$\pi_{pr}(\theta)$	prior	[-]
$\pi(\theta\|Y)$	posterior	[-]
θ	unknown parameter	[-]
ρ	density	[kg/m^3]
σ^2	variance	[-]

Subscripts

a	air
c	cold
CF	counter flow
dp	dew point
DHR	dry heat recovery unit
e	electrical energy
exh	exhaust fluid
HE	heat exchanger
h	hot
i	input
j	index
l	loss
lm	log mean
p	pump
PF	parallel flow
s	surface
supp	supply fluid
o	output
tot	total
WHR	wet heat recovery unit
∞	free stream conditions

1 Introduction

Heat exchangers are examples of distributed systems in which the dynamics in principle may be described by physical laws concerning mass, energy and momentum. One important property of heat exchangers is that the dynamic response depends upon the operating points of the massflows and temperatures. For instance, transport lags and time constants depend on massflow, and the heat transfer coefficient is a function of both temperature and massflow. This has to be accounted for in the model if it is to be valid over a wide range of operating conditions [1].

In practice, heat exchangers are devices that are used to cool or heat a fluid by exchanging thermal energy with another fluid entering at a different temperature [2]. Depending on the application, different types and geometries of heat exchangers are available on the market. Among them plate heat exchangers composed of several plates separated by empty spaces called *duct* are considered in this study.

Designing optimal heat exchanger networks has been the subject of numerous studies during the last decade [3, 4, 5]. Many methods can be found in literature for optimization problems, based on different strategies, most of the time developed for a specific class of models. In engineering applications, most of the time engineers responsible for the design of industrial devices have to face problems with more than one objective to fulfill at the same time [6].

In this Master's thesis, we consider specifically *multi-objective* optimization problems due to the fact that the goals set is to minimize the Life Cycle Cost (LCC) function which represents the price of saved energy, to minimize the heat exchanger network area together with maximizing the momentary heat recovery output at the same time, for that reason, multi-objective evolutionary algorithms are of great use. The key feature of these algorithms is that they are population based which enables them to find a diverse set of Pareto optimal solutions in a single simulation run. Having a vast interval for Pareto optimal solutions is a great advantage in order to assess different regions of attraction for a particular model parameter [7].

The considered heat recovery system is composed of two different connected heat exchangers such as dry and wet heat exchangers. The dry heat exchanger system is mainly used for heating and cooling the air fluid, while the wet heat exchanger is used for heating the water fluid. The whole system is equipped with steam heat exchangers which

provide additional energy when heat recovery capacity is not enough for example during really cold periods or other extra load situations. There are also other machines which are mainly used to pump the fluid flow through the heat exchangers. Now, the question is to find out an effective way to optimize the price of the saved energy which can be gained from the heat recovery units together with minimizing the area of the system.

Formulation of the LCC function for minimizing the price of the saved energy for the system, the cost function for minimizing the area of the system, and the cost function for maximizing the heat recovery output are given and optimized using Nondominated Sorting Genetic Algorithm II (NSGA-II) are presented in this study. After that, Markov Chain Monte Carlo (MCMC) methods are used on top of optimization results to take into account the uncertainty in the models.

This Master's thesis is divided into nine Chapters. Chapters 2, 3 and 4 give details for the background about the heat exchanger system considered in this project work, starting from the problem description, following by a brief review about structure and operating principals of dryer section heat recovery and ending with heat exchanger analysis and model description of both dry and wet heat exchangers. Chapter 5 comes up with our different optimization models and the presentation of NSGA-II algorithm. The MCMC methods and how they are used inside the optimizer are explained in Chapter 6. The implementation methodology of the case study and the main optimization and MCMC results are presented and discussed in Chapter 7 and 8 respectively. The last Chapter briefly concludes the work done.

2 Problem Description

Dryer section heat recovery has an important role in the paper machine energy economy. The purpose of dryer section is to evaporate water from the paper web, which by far is the most energy intensive unit operation of the whole paper manufacturing process. Primary energy brought to the dryer section is transferred to the surrounding drying air and removed from the dryer section. Most of this energy are recovered in dryer section heat recovery.

The dryer section consists of a sequence of heat exchangers with different heat transfer rates to different streams. Having a significant impact on the economy, this presents a challenging task to those responsible for design. For that reason, the problem to be solved in this Master's thesis is described as follows. Given are a set of exhaust fluid arranged in a vertical direction and a set of supply fluid arranged in an horizantal direction with their corresponding mass flow and target temperatures. Corresponding specific heat capacity, heat transfer coefficients and the supply energy needed for the whole system are calculated from the models describing different type of heat exchangers of the system. The physical properties for the flow rates such as dynamic viscosity, density, thermal conductivity, etc are also given. An example of a simplified case of the heat exchanger system composed of two different heat exchangers is presented in Figure 1.

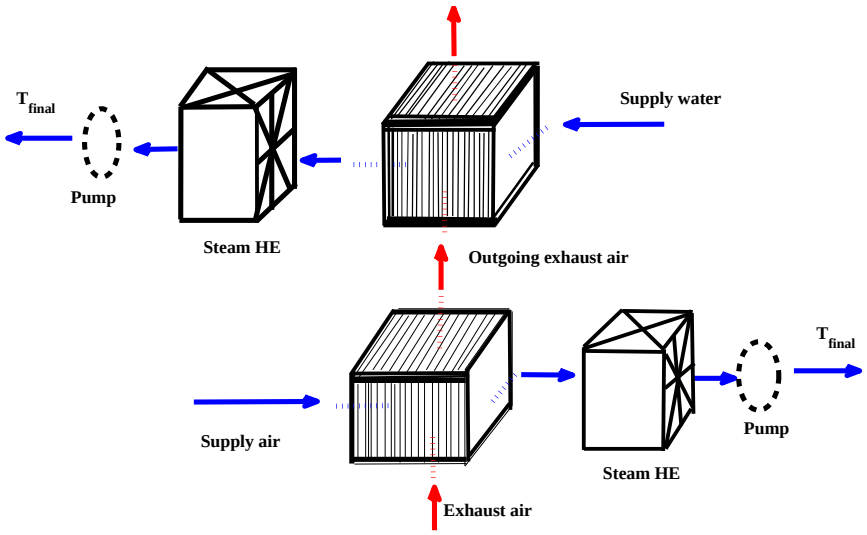

Figure 1: Example of dry and wet heat exchanger system.

In Figure 1 the first sub-process is mainly composed of an air-to-air heat exchanger without having a phase change of working fluids during the operation and is recognized as a *dry heat exchanger*, while the second sub-process is composed of an air-to-water heat

exchanger having a condensation phenomenon occurring in one of the two streams during the process of energy exchange, and is termed a *wet heat exchanger*. The two heat exchangers are connected in such a way that the outgoing exhaust fluid temperature from the dry heat exchanger is the incoming exhaust fluid temperature of the following wet heat exchanger. The current utility functions for heating different supply fluids to a desired temperature T_{final} can be deduced from the heat exchanger models described in section 4.1.3. The design of this heat recovery system must take into account investment and operation costs, space requirements, alternative heating possibilities, the permanance of the heating demand, and other mills specific characteristics.

Now the question is, how to create and to minimize the Life Cycle Cost (LCC) function which represents the price of saved energy, how to minimize the whole system network area, how to maximize the momentary heat recovery output with given constraints satisfied, and how the uncertainty in the models for the simplified case (dry heat exchanger sub-process) can be taken into account during the optimization process.

Several objectives can be specified, and these include the minimization of total costs (investment and operating costs) where the investment term includes the cost of different heat recovery units involved in the system, costs paid for heating unit in the case where heat exchangers do not produce enough energy for heating demand. The operating costs include electrical energy costs used by the pump machines and the costs paid for the additional steam energy in the process. The production process target is to minimize the current energy consumption and maximize the momentary heat recovery output.

3 Structure and Operating Principals of Dryer Section Heat Recovery

The purpose of a paper machine dryer section is to evaporate water from the paper web. The dry solids content of the web typically is about $33...55\%$ after the mechanical water removal sections and increases to $90...95\%$ in dryer section. The dominant method for evaporative process is contact drying with steam-heated cylinders as shown in Figure 2. Almost all the primary steam needed for papermaking is used in the dryer section, which makes it a very energy intensive process.

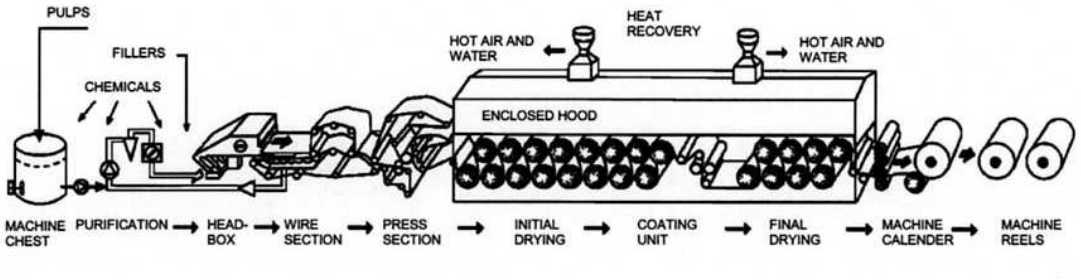

Figure 2: Fine paper machine [8].

Dryer section is separated from the surrounding machine hall with a hood to ensure optimal conditions for the drying process inside. Water evaporated from the paper web is transferred to the surrounding drying air. The humidified drying air is removed from the ceiling of the dryer hood with pumps and exhausted outside through a heat recovery system. In practice all the energy used in the dryer section is finally contained in exhaust air, which makes it an excellent source of secondary energy. The purpose of heat recovery is to transform part of this energy back to an available form.

The temperature of exhaust air from the dryer hood typically is $80...85^{o}$C and the humidity $120...180$ gH_2O/kg of dry air. The dryer hood exhaust air system has two to four heat recovery stacks depending on the amount of exhaust air. In a modern paper machine heat is recovered to hood supply air, process water, and the circulation water of machine hall ventilation. Heat recovery to white water is also possible [8]. A typical construction of a heat recovery stack is presented in Figure 3.

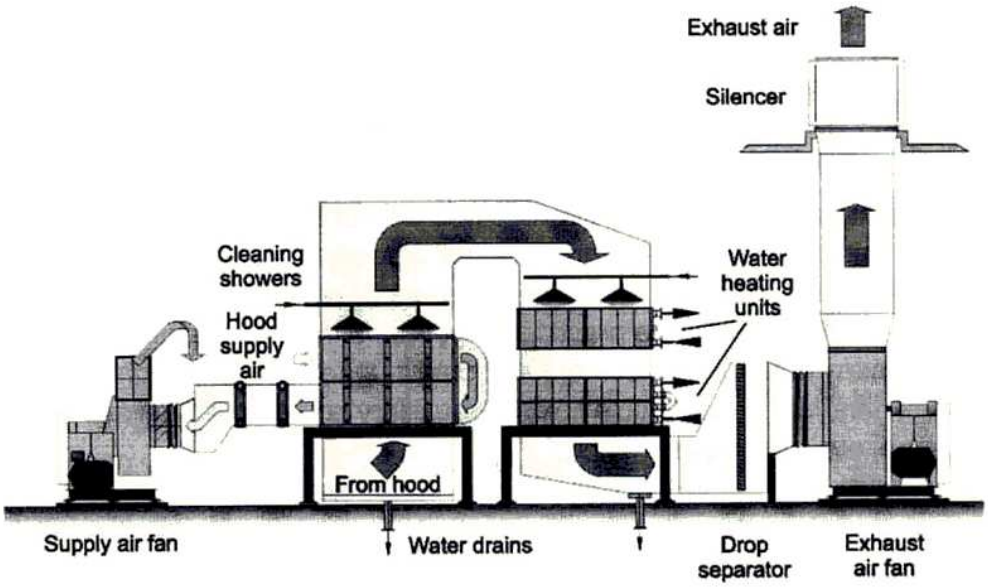

Figure 3: Heat recovery stack of a modern paper machine [8].

Modern heat recovery stacks have two types of heat exchangers. Ai-to-air heat recovery often called dry heat recovery (DHR) units because there is no condensation occuring on the hot side are used for the heating of supply air, and air-to-water heat recovery often called wet heat recovery (WHR) units because of the condensation phenomenon occuring on the surface are used for the heating of process water, circulation water, or white water.

The DHR units are crosscurrent plate heat exchangers consisting of parallel plates joined together. Exhaust air passes through in vertical and supply air in horizontal direction. Separate DHR heat exchanger units can be connected to form larger units in a combined counter- and crossflow pattern. Supply air can reach temperatures $50...60^oC$, after which heating to the final temperature 100^oC is done with steam (Steam HE). Heat transfer between exhaust air and supply air is mainly convective although little condensation may occur. The structure of DHR unit is presented in Figure 4.

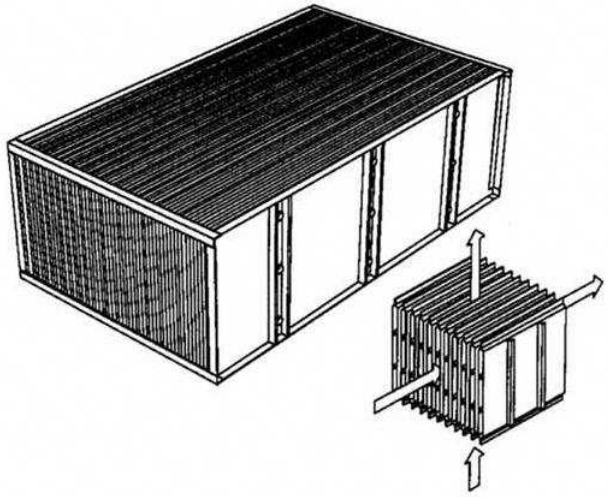

Figure 4: Dry heat recovery (DHR) unit [8].

Wet heat recovery (WHR) unit is an air-to-water heat exchanger. The WHR unit consists of a number of heat exchanger elements stacked in a frame. Water flows in counter- and crossflow pattern through channels inside plate elements, which are formed by lamellae joined together. The plate elements are connected with headers. Exhaust air passes through between the elements in vertical direction. Heat is transferred mainly by condensation on exhaust air side and by convection on water side. The units can be combined together in almost any combination [8]. The structure of a WHR heat exchanger unit is presented in Figure 5.

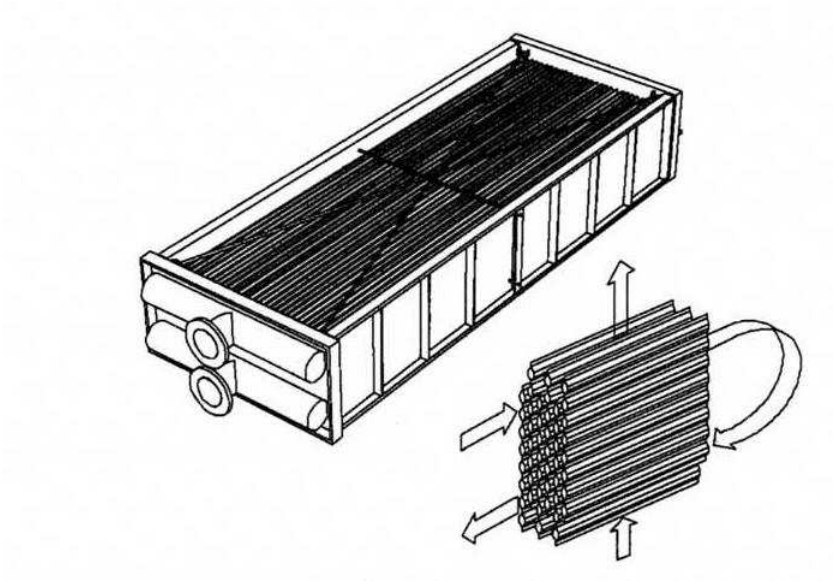

Figure 5: Wet heat recovery (WHR) unit [8].

Dryer section heat recovery is very sensitive to changes in the surroundings conditions. If

one part of the heat recovery is affected by changes, the sequential nature of the system passes the effect on to next parts. This makes the behavior of heat recovery unpredictable. The most important process variables affecting the performance of heat recovery are the mass flow rates and inlet temperatures of all the streams, and the humidity of exhaust air.

3.1 Thermodynamics of Dryer Section Heat Recovery

Energy from the humid dryer section exhaust air is transferred by several physical mechanisms. These mechanisms determine the rate of energy and the temperature levels in which heat can be recovered [8]. It is therefore, essential to understand these effects as they lay the foundation of the whole study.

Heat transfer requires the presence of temperature difference. Convection is associated with heat transfer between a surface and a fluid over the surface. Typically, the energy that is being transfered is the internal thermal energy of the fluid. Regardless of the particular nature of the convection process, the heat transfer rate equation is of the form

$$\Phi'' = \alpha(T_s - T_\infty) \tag{1}$$

where, Φ'' is the heat flux proportional to the difference between the surface and fluid temperatures T_s and T_∞, respectively. The value of convective heat transfer coefficient α depends on conditions in the boundary layer, which are influenced by a surface geometry, the nature of fluid motion and a mixture of fluid termodynamic and transport properties, i.e. the values of heat transfer coefficients depend on numerous fluid properties such as density, dynamic viscosity, thermal conductivity, specific heat, surface geometry, diffusion properties, etc [8].

The first step in the treatment of any convection problem is to determine whether the boundary layer is laminar or turbulent. In fully turbulent flow convection coefficient increases significantly compared to flow in the laminar and transition regions. A dimensionless variable determining the degree of turbulence, the Reynolds number is defined as:

$$Re = \frac{w\rho D}{\mu} \tag{2}$$

where the Reynolds number is related to the density ρ, flow rate velocity w, the dynamic viscosity of the fluid μ, and the hydaulic diameter D. The Reynolds number may be interpreted as the ratio of inertia to viscous forces in the velocity boundary layer.

The Prandtl number is the ratio of the momentum and thermal diffusivities and it is defined as

$$Pr = \frac{c_p \mu}{k} \tag{3}$$

where the Prandtl number is related to the ratio between specific heat capacity c_p, and dynamic viscousity, and the thermal conductivity k of the fluid.

The third dimensionless parameter, the Nusselt number provides a measure of the convective heat transfer occuring at the surface.

$$Nu = \frac{\alpha D}{k} \tag{4}$$

3.2 Empirical Correlations for Convection Coefficient

Heat transfer correlations can be obtained experimentally. From the knowledge of hydaulic diameter D and fluid properties, the Nusselt number, Reynolds number, and the Prandtl number can be computed from their definitions, Equations 2- 4. The results associated with a given fluid may be represented by an algebraic expression of the form

$$Nu = CRe^m Pr^n \tag{5}$$

The specific values of the coefficient C, and the exponents m and n vary with the nature of the surface geometry and type of flow. In this study the heat exhangers in dryer section heat recovery are be modeled using empirical convection correlations defined for fully turbulent flow where the Reynolds number is varying between 10^4 and 10^6.

4 Paper Machine Heat Exchangers

The process of heat exchange between two fluids that are at different temperatures and separated by a solid wall occurs in many engineering applications. The device used to implement this exchange is termed a *heat exchanger*, and specific applications may be found in space heating and air-conditioning, power production, waste heat recovery, and chemical processing.

Heat exchangers are typically classified according to *flow arrangement* and *type of construction*. The simplest heat exchanger is one for which the hot and cold fluids move in the same or opposite direction in a *concentric tube* (or *double pipe*) construction. In the *parallel-flow* type, the hot and cold fluids enter at the same end, flow in the same direction, and leave at the same end. In the *counterflow* type, the fluids enter at opposite ends, flow in opposite directions, and leave at opposite ends.

The basic designs of heat exchangers are shell-and-tube heat exchanger and plate heat exchanger, although many other configurations have been developed. Many types can be grouped according to flow layout in:

- Shell-and-tube heat exchanger (STHE), where one flow goes along a bunch of tubes and the other within an outer shell, parallel to the tubes, or in cross-flow.

- Plate heat exchanger (PHE), where corrugated plates i.e. plates formed in rows are held in contact and the two fluids flow separately along adjacent channels in the corrugation.

- Open-flow heat exchanger, where one of the flows is not confined within the equipment. They originate from air-cooled tube-banks, and are mainly used for final heat release from a liquid to ambient air, as in the car radiator, but also used in vaporisers and condensers in air-conditioning and refrigeration applications, and in directly-fired home water heaters.

- Contact heat exchanger, where the two fluids enter into direct contact [1].

This Master's thesis is dealing with plate heat exchangers which are mainly used in the current industrial project.

4.1 Heat Exchanger Analysis

To design or to predict the performance of a heat exchanger, it is essential to relate the total heat transfer rate to quantities such as the inlet and outlet fluid temperatures, the overall heat transfer coefficient, and the total surface area *A* for heat transfer. Two such relations may readily be obtained by applying overall energy balances to the hot and cold fluids. In particular, if Φ is the total rate of heat transfer between the hot and cold fluids and there is negligible heat transfer between the exchanger and its surroundings, as well as negligible potential and kinetic energy changes, then,

$$\Phi = q_{m,h}(h_{h,i} - h_{h,o}) \tag{6}$$

and

$$\Phi = q_{m,c}(h_{c,o} - h_{c,i}) \tag{7}$$

where h is the fluid specific enthalpy. The subscripts h and c refer to the hot and cold fluids, whereas i and o designate the fluid inlet and outlet conditions. If the fluids are not undergoing a phase change and constant specific heats are assumed, these expressions reduce to

$$\begin{cases} \Phi &= q_{m,h}c_{p,h}(T_{h,i} - T_{h,o}) \\ \Phi &= q_{m,c}c_{p,c}(T_{c,o} - T_{c,i}) \end{cases} \tag{8}$$

where the temperatures appearing in the expressions refer to *mean* fluid temperature at the designated locations. Note that the equations described above are independent of the flow arrangements and heat exchanger type.

Another useful expression may be obtained by relating the total heat transfer rate Φ to the temperature difference ΔT between the hot and cold fluids, where

$$\Delta T \equiv T_h - T_c \tag{9}$$

Such an expression would be an extension of Newton's law of cooling (See Appendix I), with the overall heat transfer coefficient U used in place of the single convection coeffi-

cient α. However, since ΔT varies with position in the heat exchanger, it is possible to work with a rate equation of the form

$$\Phi = UA\Delta T_m \tag{10}$$

where $\Delta T_m$is an appropriate *mean* temperature difference.

4.1.1 The Parallel-Flow Heat Exchanger

The hot and cold temperature distributions associated with a parallel-flow heat exchanger are shown in Figure 6. The temperature difference ΔT is initially large but decays rapidly with increasing x axis, approaching zero asymptotically. It is important to note that, for such an exchanger, the outlet temperature of the cold fluid never exceeds that of the hot fluid. In Figure 6 the subscripts 1 and 2 designate opposite ends of the heat exchanger. This convention is used for all types of heat exchangers considered. For parallel flow, it follows that $T_{h,i} = T_{h,1}$, $T_{h,o} = T_{h,2}$, $T_{c,i} = T_{c,1}$, and $T_{c,o} = T_{c,2}$.

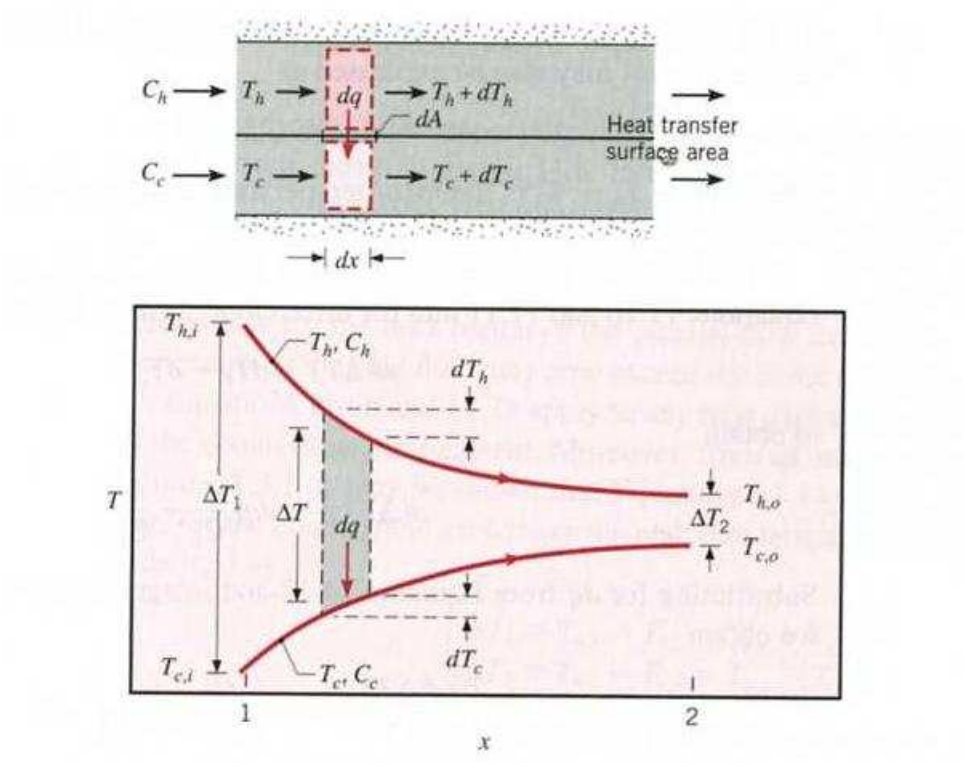

Figure 6: Temperature distributions for a parallel-flow heat exchanger [1].

The form of ΔT_m may be determined by applying an energy balance to infinitesimal elements in the hot and cold fluids. Each element is of length dx and heat transfer surface area dA, as shown in Figure 6. The energy balances and the subsequent analysis are subject to the following assumptions.

1. The heat exchanger is insulated from its surroundings, in which case the only heat exchange is between the hot and cold fluids.
2. Axial conduction along the surface is negligible.
3. Potential and kinetic energy changes are negligible.
4. The fluid specific heats are constant.
5. The overall heat transfer coefficient is constant.

The specific heats may of course change as a result of temperature variations, and the overall heat transfer coefficient may change because of variations in fluid properties and flow conditions. However, in many applications such variations are not significant, and it is reasonable to work with average values of $c_{p,c}$, $c_{p,h}$ and *U* for the heat exchanger.

After some mathematical algebra done in Appendix II the heat transfer across the surface area *A* can be be expressed as

$$\Phi = UA\Delta T_{lm} \tag{11}$$

where

$$\Delta T_{lm} = \frac{\Delta T_2 - \Delta T_1}{\ln\left(\Delta T_2/\Delta T_1\right)} = \frac{\Delta T_1 - \Delta T_2}{\ln\left(\Delta T_1/\Delta T_2\right)} \tag{12}$$

Remember that, for the *parallel-flow exchanger*,

$$\begin{cases} \Delta T_1 & = T_{h,i} - T_{c,i} \\ \Delta T_2 & = T_{h,o} - T_{c,o} \end{cases} \tag{13}$$

For more details about the derivation of *log mean temperature difference*, ΔT_{lm}, see the Appendix II.

4.1.2 The Counterflow Heat Exchanger

The hot and cold fluid temperature distributions associated with a counterflow heat exchanger are shown in Figure 7. In contrast to the parallel-flow exchanger, this configuration provides for heat transfer between the hotter portions of the two fluids at one end, as well as between the colder portions at the other. For this reason, the change in the temperature difference, $\Delta T = T_h - T_c$, with respect to x is now here as large as it is for the inlet region of the parallel-flow exchanger. Note that the outlet temperature of the cold fluid may now exceed the outlet temperature of the hot fluid.

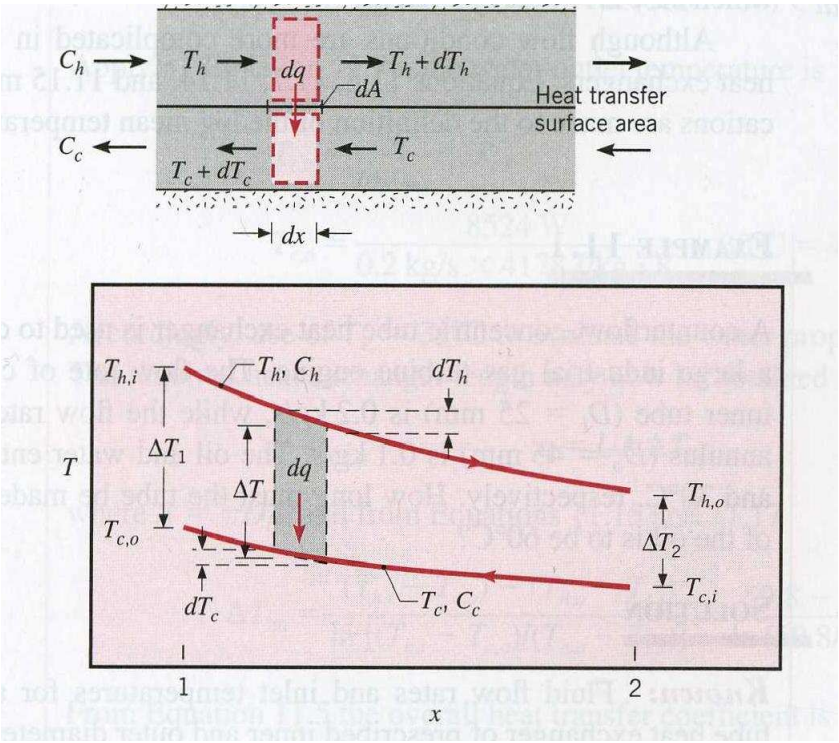

Figure 7: Temperature distributions for a counter-flow heat exchanger [1].

Equations group 8 applies to any heat exchanger and hence may be used for the counterflow arrangement. Moreover, the same analysis like that performed in the parallel-flow case is also applied in this case, it may be shown that Equations 11 and 12 also apply. However, for the *counterflow exchanger* the endpoint temperature differences must now be defined as

$$\begin{cases} \Delta T_1 & = T_{h,i} - T_{c,o} \\ \Delta T_2 & = T_{h,o} - T_{c,i} \end{cases} \tag{14}$$

Note that, for the same inlet and oulet temperatures, the log mean temperature difference for counterflow exceeds that for parallel flow, $\Delta T_{lm,CF} > \Delta T_{lm,PF}$. This is because under the special operating conditions the temperature of the hot fluid remains approximately constant throughout the heat exchanger, while the temperature of the cold fluid increases, and this affects the calculation of log mean temperature difference of both parallel and counterflow heat exchangers. Hence the surface area required to effect a prescribed heat transfer rate Φ is smaller for the counterflow than for the parallel-flow arrangement, assuming the same value U.

4.1.3 Dry and Wet Heat Exchanger Models

Heat exchangers can be applied to transfer energy between two air streams for the purpose of ventilation in air conditioning or in any other applications. In certain applications, condensation of water might occur in one of the two air streams during the process of energy exchange. In such a case, the heat exchanger is termed a *wet heat exchanger*. Conversely, a heat exchanger without having phase change of working fluids during operation is recognized as a *dry heat exchanger*. The effectiveness ϵ of a dry heat exchanger usually is expressed as a function of *number of transfer units* (NTU), and ratio of flow capacity rates (see Appendix III). Once the size and operating flow rates are determined, the heat transfer performance of a dry heat exchanger is known.

Therefore, the calculation of total heat transfer in the case of convective heat transfer without condensation occuring over the surface is given by [1]:

$$\begin{cases} \Phi &= q_{m,c} c_{p,c} (T_{c,o} - T_{c,i}) \\ \Phi &= q_{m,h} c_{p,h} (T_{h,i} - T_{h,o}) \\ \Phi &= FUA\Delta T_{lm} \end{cases} \tag{15}$$

where U is the overall heat transfer coefficient between hot and cold air fluids, and is defined as

$$\frac{1}{U} = \frac{1}{\alpha_h} + \frac{S_w}{k_w} + \frac{1}{\alpha_c} \tag{16}$$

where S_w is the thickness of heat transfer surface, k_w is the thermal conductivity of the heat transfer surface, and α_h and α_c are convective heat transfer coefficients for hot and cold fluids respectively, and

$q_{m,c}$	mass flow of cold air flow rate	[kg/s]
$q_{m,h}$	mass flow of hot air flow rate	[kg/s]
$c_{p,c}$	specific heat capacity of cold air flow rate	[kJ/kgK]
$c_{p,h}$	specific heat capacity of hot air flow rate	[kJ/kgK]
$T_{c,i}$	incoming cold air temperature	[^{o}C]
$T_{c,o}$	outgoing cold air temperature	[^{o}C]
$T_{h,i}$	incoming hot air temperature	[^{o}C]
$T_{h,o}$	outgoing hot air temperature	[^{o}C]
A	surface area of heat exchanger	[m^2]
U	overall heat transfer coefficient between streams	[W/m^{2}K]
ΔT_{lm}	log mean temperature difference for counterflow heat exchanger	[^{o}C]
F	correction factor	[-]

F is used to scale log mean temperature difference calculated by assumption of counter-flow heat exchanger to cross flow or multi-pass configuration [1].

The heat transfer process in a wet heat exchanger is much more complicated than that in a dry heat exchanger. The effectiveness of wet heat exchangers so far has not been clearly defined. The heat transfer performance of a wet heat exchanger is not only related to its geometric size and operating flow rates, but also to its temperatures and humidity ratios [9].

In the case of condensation, the effect of latent heat must be included in the model. Condensation occurs when the temperature of a vapor is reduced below its saturation temperature. If a surface has a lower temperature than the dew point, the latent energy of the vapor is released, heat is transferred on the surface, and condensate is formed. Regardless of whether it is in the form of a film or droplets, the condensate provides a resistance to heat transfer between the vapor and the surface.

If the humid air is marked with index 1, the surface of the heat exchanger on the air side with index s, and the fluid on the other side with index 2, the heat transfer rate in condensation can be written as follows [8]:

$$\Phi = \alpha_1 A_1 (T_1 - T_s) + \dot{m}_c'' A_1 l(T_s) = \frac{A_2}{\frac{S}{\lambda_s} + \frac{1}{\alpha_2}} (T_s - T_2) \tag{17}$$

where the α_1 is the convection coefficient of humid air, A_1 the surface area on the humid air side, T_1 the temperature of humid air, T_s the surface temperature on the humid air side, $\dot{m}_c''$ the mass flux of condensation on the humid air side, l the latent heat of condensation, A_2 the surface area of the fluid 2 side, S the thickness of the heat exchanger surface, λ_s the thermal conductivity, α_2 the convection coefficient of flow 2, and T_2 the temperature of fluid 2 side. The detailed description about the wet heat exchanger models can be found in [8, 10, 11].

4.2 Calculation of Pressure Drop

To transfer the supply fluid between sub-processes a suitable heat exchanger network design is needed. Dimensioning of the heat recovery system is based on the following main parameters which are valid for both dry and wet heat recovery units:

- Incoming and outgoing exhaust fluid temperatures
- Incoming and outgoing supply fluid temperatures
- Supply mass flow
- Exhaust mass flow
- Maximum allowable pressure drop over the heat recovery units

To dimension the heat recovery system the entire dimensioning topology has to be designed. This kind of complex system can be solved by the following rules [12].

- Mass flow of the exhaust air is the same in all heat recovery units

$$q_{m,1} = q_{m,2} = q_{m,3} = ... = q_{m,i} \tag{18}$$

where $q_{m,i}$ is the mass flow of the exhaust air for the heat recovery unit i.

- Total head loss through the system equals the sum of head loss in each heat recovery unit

$$\Delta P_{tot} = \sum_{i=1}^{n} \Delta P_i \tag{19}$$

where

ΔP_{tot}	total pressure drop over the entire system	[Pa]
ΔP_i	pressure drop over the heat recovery unit i	[Pa]

Furthermore, the pressure loss for each part of the system can be calculated as follows:

$$\Delta P_i = \frac{V_i^2}{2g} \left(\frac{f_i L_i}{d_i} + \sum K \right) \tag{20}$$

where

f_i	friction factor for the surface i	[-]
$\sum K$	sum of loss coefficients for the heat recovery unit i	[-]
L_i	length of the surface i	[m]
g	gravitational acceleration	[m/s^2]

The calculation of pressure drop for the heat recovery unit has two sides. On both exhaust and supply fluid directions, the pressure drop over the heat recovery unit is the sum of the pressure drop at the entrance of the duct, pressure drop along the duct and the pressure drop at the exit of the duct.

5 Optimization Models and Techniques

Optimization is the process of making something better. An engineer or scientist conjures up a new idea and optimization improves on that idea. Optimization consists of trying variations on an initial concept and using the information gained to improve on the idea.

Optimization can be distinguished by either discrete or continuous parameters. Discrete parameters have only a finite number of possible values, whereas continuous parameters have an infinite number of possible values. Discrete parameter optimization is also known as combinatorial optimization, because the optimum solution consits of certain combination of parameters from a finite pool of all possible parameters. However, if we are trying to find the minimum value of $f(x)$ on real axis, it is more appropriate to view the problem as continuous.

Parameters often have limits or constraints. Constrained optimization incorporates parameter equalities and inequalities into the cost function. Unconstrained optimization allows the parameters to take any value. A constrained parameter often converts into an unconstrained parameter through a transformation of variables. Some algorithms try to minimize the cost by starting from an initial set of parameter values. These minimum solvers or algorithms easily get stuck in local minima but tend to be fast. Therefore, they are the traditional optimization algorithms and are generally based on calculus methods [13].

5.1 Optimization Models

In an optimization problem, the main goal is to optimize (maximize or minimize) one or several cost functions $f_m(X)$ which depend on several variables

$$\mathrm{X} = (\mathrm{x}_1, x_2, \ldots, x_n)$$

These are called control variables because the function value can be controlled with them by choosing their values. In many problems the choice of values of X is not totally free but is subject to some constraints, that, is, additional conditions arising from the nature of the problem and the variables.

In this Master's thesis, the optimization problem has three sides:

- Optimize the LCC function which represents the price of saved energy
- Optimize the structure of the system during the design stage
- Optimize the system output during the process operation

The optimization premise for design is to minimize the Life Cycle Costs (LCC) related to the saved energy of the system. For a production process the target is to minimize the current energy consumption and to maximize the momentary heat recovery output.

5.2 Life Cycle Cost (LCC)

Life cycle costing is an economic assessment of an item, system, or facility over its life time, including the initial purchase price of the equipment and the annual operating expenses, expressed in equivalent Euros. The primary objective of life cycle costing is providing input into decision making in any or all phases of a product's life cycle. Another important objective in the preparation of LCC models is to identify costs that may have a major impact on the LCC or may be of special interest for that specific application.

Life cycle costing is used to compare various options by identifying and assessing economic impacts over the life of each option. LCC can also be used to assess the consequences of decisions already made, as well as to estimate the annual operation and maintenance costs for budgeting purposes. Life cycle costs include the value of purchase and installing costs, maintenance costs, energy consumption, and disposal costs over the life span of a facility or service. Life cycle costs are summations of cost estimates from inception to disposal for both equipment and projects as determined by an analytical study and estimate of total costs experienced during their life.

The most popular technique used for evaluating the profitability of any investment is Life Cycle Cost Analysis (LCCA) which is defined as a cost-centred engineering economic analysis. The purpose of LCCA is to estimate the overall costs of project alternatives and to select the design that ensures that facility will provide the lowest overall cost of ownership consistent with its quality and function. The objective of LCCA is to choose the most cost effective approach from a series of alternatives so that the least long term

cost of ownership is achieved. LCCA helps to justify equipment and process selection based on total costs rather than the initial purchase price.

During the LCCA both present and future costs should be taken into account and related to one another, when making decision. Today's Euro is not equal to tomorrow's Euro. A current Euro is worth more than the prospect of an Euro at some future time. The amount of future worth depends on the investments rate and the length of time of the investment. A key element in life cycle costing is an assessment using equivalent Euros. Inflation is also an important consideration in life cycle costing because of the effect it has on the costs. The life cycle, over which the costs are projected, also influences the value of the Life Cycle Cost. Therefore, the present value factor may be used to determine the present value of a future amount of money and it is calculated as follows [14]:

$$P = \frac{F}{(1+r)^t} \tag{21}$$

where

P	present amount of money	[EUR]
F	future amount of money to be discounted	[EUR]
r	real interest rate	[%/a]
t	life cycle or period	[a]

The present amount of money may also be calculated as:

$$P = A\frac{a(a^t - 1)}{a - 1} \tag{22}$$

where

A	amount of money to be discounted	[EUR]
a	escalation factor	[-]

Since the duration of project extends over several years, it is necessary to have a method of taking into account the uncertainty in the market price of the equipments to be used in the project that might be occur in the future. This is where the escalation factors are used. In other words, the escalation factor is a financial factor used to take into account the uncertainty in the market price of any product which might occur in the future, and it

can be calculated as follows:

$$a = \frac{1+i}{1-r} \tag{23}$$

where i is the escalation rate.

As it was mentioned earlier an effective way to analyze the profitability of the investment for a heat exchanger system with heat recovery is to use the Life Cycle Cost Analysis (LCCA) and create the total LCC function for the system and try to minimize that. In this type of system including heat recovery the target function is created by setting the LCC costs to be equal with the present value of the saved energy which will represent the price of the saved energy. The main target is to get the created LCC function to give cheaper energy price than the same LCC function done for the system using primary energy. In this context the target function for optimization can be specified as follows [15]:

$$\min \left\{ \frac{LCC}{a' E_p} \right\} \tag{24}$$

where

a'	present value factor which takes inflation into account	[-]
E_p	totally recovered energy	[kWh]

Life Cycle Cost for the system includes the investments, energy, maintenance costs and other costs. Additionally the LCC-term has to include the possible investment or the taxation subventions and the incomes. If maintenance and running costs differ between alternatives they have to be counted into the expenses as well. The observation period for LCC is the total life span of the system. The general LCC function for the heat exchanger system with heat recovery can be formulated as follows:

$$LCC = \sum_{t=0}^{t_{lifespan}} \frac{1}{(1+r)^t} I_t + a_e'' e_e E_e + a_h'' e_h E_h + a' K \tag{25}$$

where

I_t	investment done to the system at time t	[EUR]
r	real interest rate	[%/a]
$a_e^{''}$	escalation term for electrical energy	[%/a]
$a_h^{''}$	escalation term for heat energy	[%/a]
e_e	electric energy price at the base date	[EUR/kWh]
e_h	heat energy price at the base date	[EUR/kWh]
E_h	consumed heat energy	[kWh]
E_e	consumed electric energy	[kWh]
K	Annual maintenance costs of the system	[EUR/a]

The cost functions for different solutions include frequently the terms which are equal between variants. If the target is to find only the best solution among all alternatives the constant terms can be neglected. If the target is to derive the absolute value for example for the price of saved energy then all terms have to be taken into account. This study is used the approach where part of the model elements are assumed to be the same in spite of the system size and thus neglected. These assumptions are:

1. Investment is to be done in any case, this means that the constant variables can be neglected.
2. Maintenance costs are equal, this means that $a^{'}K = 0$

With these assumptions the LCC-term in Equation 25 reduces to the form:

$$LCC = \sum_{t=0}^{t_{lifespan}} \frac{1}{(1+r)^t} I_t + a_e^{''} e_e E_e + a_h^{''} e_h E_h \tag{26}$$

To solve the components for Equation 26 the simulation models have to be translated as cost functions. Generally it can be concerned that the cost functions for sub-models are all similar type so that is proportional to the total mass of the unit dimensioned with the simulation model. From the practice it is known that this assumption is valid when operating with the heat recovery units which have approximately standard dimensions and operating parameters. This assumption leads to the connection that the needed surface area or the control volume is directly correlated with the mass of the heat recovery unit. Now the model is simplified furthermore with the following assumptions:

1. Material thickness is constant in spite of system size, this means that $m_{unit} = f(A_{unit})$

2. Installation of the system does not depend on the system size, this means that the investment at year zero (I_0) will be composed purely based on the material and equipment prices.

3. The cost for heating surface (heating coil) is indirectly proportional to the size of the main heat recovery unit and it is part of the investment term, i.e. $I_{0,coil} = C_{coil}(E_h - E_p)$ where C_{coil} is a constant which scales the price of heating surface.

4. The cost of steam heating is also indirectly proportional to the size of the main heat recovery unit, i.e. $Cost_{steam} = C_{steam}(E_h - E_p)$ where C_{steam} is a constant which scales the price of steam heating. This should be included in the investment term, too, but it is included in the operating cost term in this case.

5. The cost of electricity consumed by the system during the operating time is also part of the operating cost term.

The annual saved energy E_p located in the function divider can be calculated as follows [16]:

$$E_p = \int_0^{t_{oper}} \Phi_{HR} dt \tag{27}$$

where Φ_{HR} is the heat recovered energy from the heat recovery units of the system. By putting these formulas together the complete target function for the optimization can be specified as follows:

$$\min \left\{ \frac{\sum_{t=0}^{t_{lifespan}} \frac{1}{(1+r)^t} I_t + a_e'' e_e E_e + a_h'' e_h E_h}{a' \int_0^{t_{oper}} \Phi_{HR} dt} \right\} \tag{28}$$

During the production process, the main energy consumers in the heat exchanger system are heating of the supply air in a dry heat exchanger sub-process and heating of the supply water or whatever fluid in a wet heat exchanger sub-process. Annual energy consumption for fluid heating can be calculated from the equation:

$$E_h = q_{m,fluid} c_p \int_0^{t_{oper}} (T_{fluid} - T_{in})\, dt \tag{29}$$

In many cases T_{fluid} can be assumed to be constant year around. T_{in} is the incoming temperature of the flow rate.

5.3 Combination of Simulation and Optimization

The starting point of this study is an existing heat recovery system, for which all possibilities to improve efficiency are investigated. This includes changing the structure of heat recovery as well as its operation point. A simulation tool, which enables comparison between the performance of heat recovery in its current and changed operational or structural situations, is needed. This can be done with thermodynamic modeling.

The thermodynamic modeling part for the heat recovery units used in this study was done in [11] and the thermodynamic models are created with Matlab software. There are two developed main functions, named Dry Heat Recovery (DHR) and Wet Heat Recovery (WHR) according to the type of heat exchanger they represent. Any heat recovery system can be simulated at any operation point by connecting the DHR and WHR units with each other in a desired way. The inlet conditions of all the streams and the exact structure of the heat recovery system has to be known. The programs calculate the outlet temperatures of all the streams, heat transfer, surface area of heat exchangers, changes in the exhaust air humidity inside the heat exchangers etc.

During the design optimization, the presented optimization problem can be solved unconstrained and all the parameters affecting to the system operation can be arranged to give the most optimal solution. However, due to the mechanical limitations and also due to some experimental facts it is better to limit the worst and impossible solutions out and avoid useless calculation. This is especially important when the model itself is complicated and needs a lot of CPU-time. In this context it is important to notice that many of the limitations are not constraints for the mathematical optimization but assumptions for the model itself. Difference between these is remarkable because the constraints affect to the optimization algorithm and the assumptions to the simulation model.

The presented model contains several parameters which can be adjusted. These parameters vary depending on the model usage, i.e. the operator optimizing design of the system or optimizing the production operation. In Figure 8 is presented the complete model where all the parameters are to be subject to optimization. The simplifications for these

are presented for the current model in the implementation part.

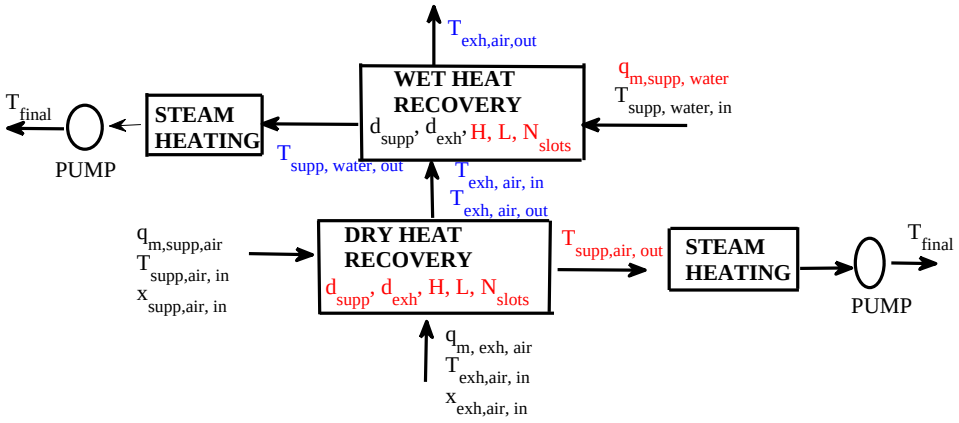

Figure 8: Parameter table for design optimization (Red : Control variable, Blue: Variable, Black = Constant).

where

d_{exh}	slot size on exhaust fluid side	[m]
d_{supp}	slot size on supply fluid side	[m]
L	plate size on supply fluid side	[m]
H	plate size on exhaust fluid side	[m]
N	number of slots inside the heat recovery unit	[-]
x	amount of humid air in the fluid	[gH_2O/kg]

The subscripts exh and $supp$ indicate the exhaust and supply fluid respectively. After the model is created by optimizing the physical parameters according to known starting values the model can be modified and used for the operational optimization, too. This means that part of the simulation model parameters (geometry parameters) are set constant based on dimensioning and during the daily operation the process parameters are tuned to produce the optimal system output. The optimization function can also in this case be LCCA based, but practical approach is to create a function maximizing available momentary output of the heat recovery during the observation period, together with a function minimizing the total area of the heat recovery units involved in the whole system given the geometry constraints satisfied. In this case the target function will be:

$$\begin{cases} \max \Phi_{HR} \\ \min A_{HR} \end{cases} \tag{30}$$

subject to

$L.B \leq$ geometry parameters $\leq$U.B

Where $L.B$ and $U.B$ are the lower and upper bounds of the given geometry parameters respectively.

5.4 Genetic Algorithm (GA)

Over the last decade, genetic algorithms (GAs) have been extensively used as search and optimization tools in various problem domains, including the sciences, commerce and engineering. The primary reasons for their success are their broad applicability, ease of use and global perspective [17].

The concept of a genetic algorithm was first conceived by John Holland of the University of Michigan, Ann Arbor. Thereafter, he and his students have contributed much to the development of this field.

Genetic algorithms (GA) are based on principles from genetics and evolution. GAs can be used to solve optimization problems. GAs are one example of mathematical technology transfer: by simulating evolution we are actually able to solve optimization problems from a variety of sources. Instead of a single sample from the solution space, GAs maintain a population of vectors. New solution vectors are generated using selection, recombination and mutation. The new vectors are evaluated for their fitness, and the old population is replaced with a new one. This is repeated until the algorithm converges or runs out of time or patience. If the search space of all possible solutions is big enough, we may be satisfied with a solution which is better than a random guess [18].

The general form of a GA can be summarized as follows:

1. Start with a random generation of an initial population of N chromosomes

2. Carry out a fitness evaluation, $f(x)$, for each x chromosome forming the population

3. Apply a crossover operation to the population in order to generate a new one according to the following steps:

- Select two parent chromosomes according to their best fitness.

- Use a crossover probability in order to reproduce the two parents into two new chromosomes (offspring's). Note that if crossing the parents is not carried out, then the offspring's become an exact replica of their parents.

- Use a mutation probability to modify the new chromosomes.

- Relocate the new chromosomes in the population space.

4. Use this new population for continuing searching the best solution, i.e.continue the execution of the algorithm.

5. Carry out a test for satisfying a convenient convergent criterion, if this condition is achieved stop the procedure and select the chromosome that has the best fitness as the solution of the problem.

6. If Step 5 is not satisfied then go back to step 2 [19].

5.4.1 Multi-Objective Genetic Algorithm (MOGA)

In principle, multiple objective optimization problems are very different from single-objective optimization problems. In the single-objective case, one attempts to obtain the best solution, which is absolutely superior to all other alternatives. In the case of multiple-objectives, there does not necessarily exist a solution that is best with respect to all objectives because of incommensurability and conflict among objectives. A solution may be best in one objective but worst in other objectives. Therefore, there usually exist a set of solutions for the multiple-objective case which cannot simply be compared with each other. For such solutions, called nondominated solutions or Pareto optimal solutions, no improvement in any objective function is possible without sacrificing at least one of the other objective functions [20].

Fonseca and Fleming (1993) first introcuded a multi-objective GA which used the non-dominated classification of a GA population. The investigators were the first to suggest a multi-objective GA which explicitly caters to emphasize nondominated solutions and simultaneously maintains diversity in the nondominated solutions [17].

5.4.2 Elitist Nondominated Sorting Genetic Algorithm II (NSGA-II)

Nondominated Sorting Genetic Algorithms (NSGA) is a popular nondomination based genetic algorithm for multi-objective optimization. It is a very effective algorithm but has been generally criticized for its computational complexity, lack of elitism (combining the parent and offspring populations during the selection operation) and for choosing the optimal parameter value for sharing parameter σ_{share}. A modified version, NSGA-II was developed, which has a better sorting algorithm, incorporates elitism and no sharing parameter needs to be chosen a priori [21].

The elitist nondominated sorting genetic algorithm II (NSGA-II) is used in this study to obtain Pareto-optimal solutions. This is a robust algorithm and incorporates the concept of elitism to make it more powerful than earlier algorithm, NSGA. The MOGA used in this study is NSGA-II whose its flowchart is given in Figure 9.

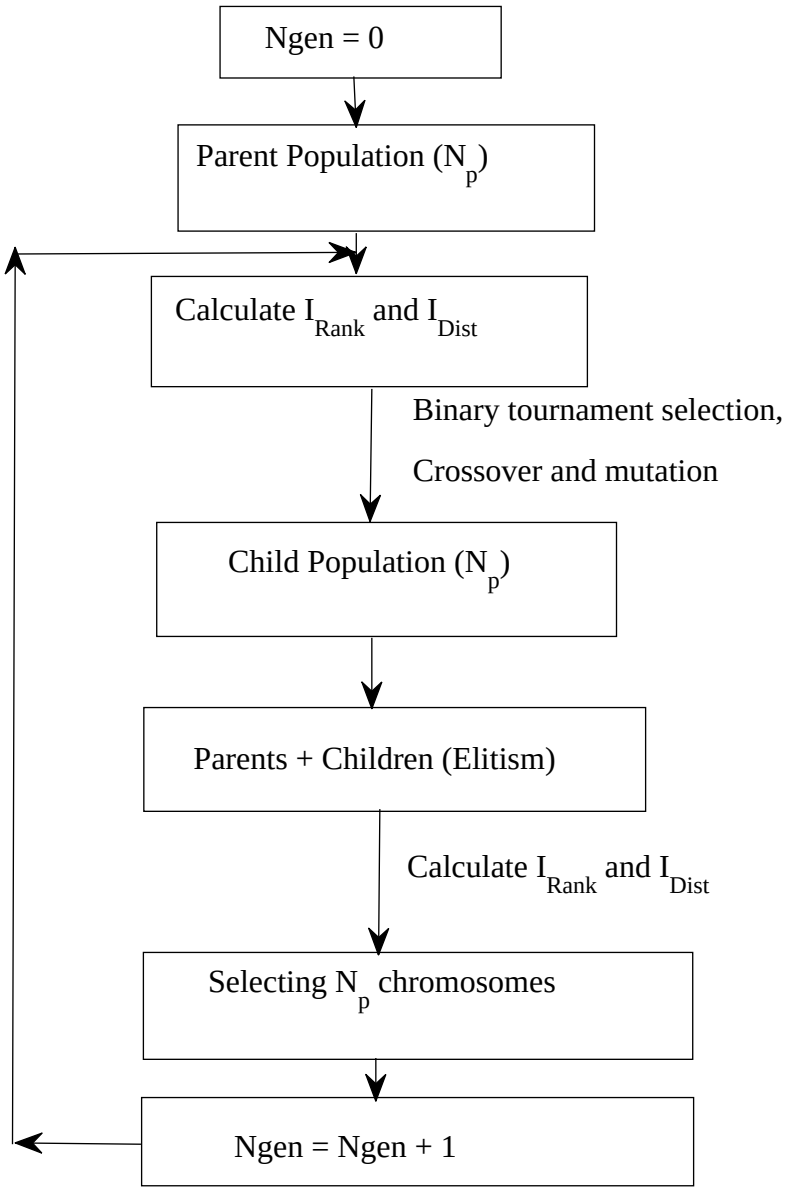

Figure 9: Flowchart for NSGA-II.

Elitist Nondominated Sorting Genetic Algorithm, NSGA-II

1. Population Initialization.
   The population is initialized based on problem range and constraints if any, i.e. generate box, P, of N_p parent chromosomes.

2. Nondominated sort.

The initialized population is sorted based on nondomination i.e chromosomes are classified into $fronts$ based on nondomination as follows:

- Create new (empty) box, $P^{'}$, of size, N_p.
- Transfer i_{th} chromosome from P to $P^{'}$, starting with the first.
- Compare chromosome i with each member, e.g., j, in $P^{'}$, one at a time.
- If i dominates over j, remove j from $P^{'}$ and put back in P.
- If i is dominated by j, remove i from $P^{'}$ and put back in P.
- If i and j are nondominating, keep both i and j in $P^{'}$. Continue for all j.
- Repeat for all chromosomes in P. $P^{'}$ constitutes the first $front$ of sub-box (of size $\leq N_p$) of nondominated chromosomes. Assign it $Rank$= 1.
- Create subsequent fronts in (lower) sub-boxes of $P^{'}$ using the chromosomes remaining in P. Compare these members $only$ with members present in the $current$ sub-box. Assign these $Ranks = 2, 3, \ldots$. Finally, we have all N_p chromosomes in $P^{'}$, boxed into one or more fronts.
  This sequential procedure is superior to that used in NSGA where any chromosome is compared to all other $N_p - 1$ chromosomes.

3. Crowding Distance (See Appendix IV.).
   Once the nondominated sort is complete the crowding distance is assigned. Since the individuals are selected based on rank and crowding distance all the individuals in the population are assigned a crowding distance value. Evaluate the crowding distance, $I_{i,dist}$, for the i_{th} chromosome in any front:

   - Rearrange all chromosomes in front j in ascending order of the values of any one of their fitness functions, F_i.

- Find the largest cuboid (rectangle for 2 fitness functions) enclosing i that just touches its nearest neighbors in the $F-$space.

- $I_{i,dist} \equiv \frac{1}{2}$(sum of all sides of this cuboid).

- Assign large values of $I_{i,dist}$ to solutions at the boundaries.
  This helps maintain diversity in the Pareto set. This procedure is superior to the sharing operation of NSGA.

4. Selection.
   Copy the best of the N_p chromosomes of $P^{'}$ in a new box, $P^{''}$ ($best\ \ parents$):

   - Select any pair, i and j, from $P^{'}$ (randomly, irrespective of fronts).

   - Identify the better of these two chromosomes, i is better than j if

   $$\mathrm{I}_{i,rank} \neq I_{j,rank} : I_{i,rank} < I_{j,rank}$$
   $$\mathrm{I}_{i,rank} = I_{j,rank} : I_{i,dist} > I_{j,dist}$$

   - Copy (without removing from $P^{'}$) the better chromosome in a new box, $P^{''}$. Repeat till $P^{''}$ has N_p members.

   - Copy all of $P^{''}$ in a new box, D, of size N_p. Not all of $P^{'}$ need be in $P^{''}$ or D.

5. Genetic Operators.
   Carry out crossover and mutation of chromosomes in D. This gives a box of N_p daughter chromosomes.

6. Recombination and Selection.
   The offspring population is combined with the current generation population and selection is performed to set the individuals of the next generation.
   Copy all the N_p best parents ($P^{''}$)and all the N_p daughters (D) in box PD (*elitism*). Box PD has $2N_p$ chromosomes.

7. Reclassify these $2N_p$ chromosomes into fronts (box $PD^{'}$) using *only* nondomination.

8. Take the best N_p from box $PD^{'}$ and put into box $P^{'''}$.

9. This complete one generation. Stop if criteria are met.

10. Copy $P^{'''}$ into starting box, *P*. Go to Step 2 above [22].

6 Markov Chain Monte Carlo Methods in Optimizing a Heat Exchanger Network

Even though the optimal design parameters can be found using multiobjective optimization methods, the interpretation of results as statistical analysis is arguably more useful, since as well as identifying the most likely parameters, it is essential to assess the uncertainty associated with these estimates. Error estimates are not easily available within the optimization paradigm, yet they are a natural product of proper statistical inference [23]. In addition, Markov Chain Monte Carlo (MCMC) methods allow the combination of both quantitative and qualitative information, i.e., combine plate heat exchanger data with the intuitive knowledge and experience of heat exchanger practitioners (via prior distributions: our beliefs about the phenomenon beforehand). This Chapter is introduced by a closer look on Bayesian inference in parameter estimation, prior distributions, and ending with description of MCMC methods.

6.1 Bayesian Inference in Parameter Estimation

The general form on nonlinear model is presented in Equation 31. The model consists of measurements Y, known quantities X (constants, control variables, etc), unknown parameters θ, and measurement erros ϵ.

$$Y = f\left(X, \theta\right) + \epsilon \tag{31}$$

The problem is to estimate the unknown parameters θ based on the measurements Y. This problem can be solved by different numerical methods based on random sampling presented in the framework of Bayesian theory. That is, the error and the unknown parameters in the model are random and have a distribution, they are not thought to have a single ”correct” value, but different possible values, others being more probable than the others [24].

In statistical analysis there are two major approaches to inference, the Frequentist and the Bayesian approach. In general, the goal in statistical inference is to make conclusions about a phenomenon based on observed data. In the Frequentist framework the observations made in the past are analyzed with a created model and the result is regarded as confidence about the state of the real world. That is, we assume that the phenomenon

modeled has a statistical stability: the probabilities are defined as frequencies with which an event occur if the experiment is run many times. An event with probability p is thought to occur pn times if the experiment is repeated n times.

In the Bayesian approach the interpretation of probability is subjective. The belief quantified before is updated to present belief through new observed data. In the Bayesian framework the probability is never just a frequency (single value), but a distribution of possible values. In the previous example the frequency pn can have different values of which other are more probable than others, for a every claim a probability can be assigned that tells how strong our belief about the claim is. That is, the Bayesian inference is based on assigning degrees of beliefs for different events.

A common task in statistical analysis is the estimation of the unknown model parameters. The Frequentist approach relies on estimators derived from different data sets (experiments) and a specific sampling distribution of the estimators. In the Bayesian approach the solution encompasses various possible parameter values. Therefore, the Bayesian approach is by nature suitable for modeling uncertainty in the model parameters and model predictions.

The Bayesian approach is based on *prior* and *likelihood* distributions of parameters. The prior distributions include our beliefs about the problem beforehand, whereas the likelihood represents the probabilities of observing a certain set of parameter values. The prior and the likelihood are updated to a posterior distribution, which represent the actual parameter distribution conditioned on the observed data, through the Bayesian rule [25].

6.1.1 Bayes' Rule

As stated above, the Bayesian solution to the parameter estimation task is the posterior distribution of the parameters, which is the conditional probability distribution of the unknown parameters given the observed data. That is, we are interested in the distribution with probability density function $\pi(\theta|Y)$ where θ denotes the unknown parameter values and Y contains the observations.

To define $\pi(\theta|Y)$ we assume that there is a joint probability density function $p(\theta|Y)$ that gives the probability for every combination of parameters and data. In the Bayesian framework this function is expressed as

$$p(\theta|Y) = p(Y|\theta)\pi_{pr}(\theta) \tag{32}$$

where π_{pr} is the prior distribution that describes our prior knowledge of the parameters. Here $p(Y|\theta)$ is the likelihood function that gives the probability of receiving data Y if we have parameter value θ. In order to receive the probability density function the joint probability has to be normalized so that the probabilities sum to value 1. This scaling factor is the density function of all possible measurements, $p_Y(Y)$. The posterior density can now be written in a form of the Bayesian rule [26]:

$$\pi(\theta|Y) = \frac{p(Y|\theta)\pi_{pr}(\theta)}{p_Y(Y)} \tag{33}$$

which is analogous to the Bayesian rule from the elementary probability calculus for two random variable A and B:

$$P(A|B) = \frac{P(A \cap B)}{P(B)} = \frac{P(B|A)P(A)}{P(B)} \tag{34}$$

The scaling factor (the marginal density of observations) can be calculated as the sum (integral) over all possible joint probabilities. That is, the Bayesian formula can be expressed with

$$\pi(\theta|Y) = \frac{p(Y|\theta)\pi_{pr}(\theta)}{\int_{\Re^d} p(Y|\theta)\pi_{pr}(\theta)d\theta} \tag{35}$$

The tricky part in implementing Bayesian inference in practice is the normalizing constant that requires integration over an often high-dimensional space. This integral is seldom possible to calculate analytically. Deterministic methods based on the discretization of the space may not be feasible because of large computational complexity due to high dimension. This problem can be solved, for example, with Monte Carlo (MC) integration

methods or with Markov Chain Monte Carlo (MCMC) methods in which the need for computing these difficult integrals vanishes.

Before moving into MCMC methods in parameter estimation, we take a closer look on the role of prior and likelihood distributions from the point of view of parameter estimation.

6.1.2 Prior Distributions

As mentioned, the prior distribution describes our previous (a priori) knowledge about the unknown parameters in the model. With properly selecting the prior distribution we can emphasize the parameters that we know to be more probable than the others.

If we do have any a priori knowledge about the parameters, an *uninformative prior* can be used. This is, we state $\pi_{pr}(\theta) = 1$. If we have limits for the parameters, we can assign a uniform prior for the parameters in the feasible interval [25].

For informative priors it is often useful to use so called conjugate priors. This means that both the prior and the posterior come from the same family of distributions. Conjugate priors can be found, for example, for exponential and Gaussian (normal) distributions.

6.1.3 Likelihood in Parameter Estimation

As said, in the Bayesian framework the error term in Equation 31 is distributed according to some distribution that has some probability density function (PDF), say p_ϵ. If we assume that the measurement error is independent of θ, it can be shown that the difference between the measurements and predicted values is distributed in the same way as the error. That is, the likelihood can be written as

$$p(Y|\theta) = p_\epsilon(Y - f(X, \theta)) \tag{36}$$

If we assume that the measurement noise is Gaussian with mean zero and covariance C, that is, $\epsilon \sim N(0, C)$, the likelihood can also be written as the Gaussian PDF for the difference between measurements and obervations:

$$p(Y|\theta) = \frac{1}{(2\pi)^{n/2}(\det C)^{1/2}} e^{-0.5(Y-f(X,\theta))^T C^{-1}(Y-f(X,\theta))} \tag{37}$$

Especially, if we assume that the error terms $\epsilon_i = Y_i - f(X_i, \theta)$ (measurement error for measurement i) are independent and normally distributed, that is $\epsilon_i \sim N(0, \sigma^2)$ and $\epsilon \sim N(0, \sigma^2 I)$, the likelihood for a certain measurement gets the form

$$p(Y|\theta) = \frac{1}{(2\pi\sigma^2)^{1/2}} e^{-0.5\sigma^{-2}(Y_i - f(X_i,\theta))^2} \tag{38}$$

Since the error terms are assumed to be independent, the combined likelihood of all the measurements can be written as a product

$$p(Y|\theta) = \prod_{i=1}^{n} p(Y_i|\theta) = \frac{1}{(2\pi\sigma^2)^{n/2}} e^{-0.5\sigma^{-2} SS_\theta} \tag{39}$$

where $SS_\theta = \sum_i (Y_i - f(X_i, \theta))^2$. This is the basis of the practical implementations. Note that if measurement errors in different points are identically distributed or if correlations between error terms exist, the PDF has to be written in full form (Equation 35).

When using an uninformative prior $\pi_{pr}(\theta) = 1$, also the posterior is known up to the normalizing constant (integral). That is,

$$\pi(\theta|Y) \propto p(Y|\theta) \tag{40}$$

6.1.4 Point Estimates

We are often interested, besides in the shape of the posterior distribution, in getting some values that in some sense represent the posterior distribution. We can take the ”most probable” values of the posterior density that leads to *maximum a posteriori* (MAP) [27]:

$$\widehat{\theta}_{MAP} = \max_{\theta} \ \pi(\theta|Y) \tag{41}$$

For the MAP estimate we normally used the unnormalized posterior $\pi(\theta|Y) \propto p(Y|\theta)\pi_{pr}(\theta)$, since it is simple to evaluate and results to same estimate. Now,

$$\widehat{\theta}_{MAP} = \max_{\theta} \ p(Y|\theta)p(\theta) \tag{42}$$

If we use the non informative prior, the task of finding the MAP reduces to finding the Maximum Likelihood (ML). The estimate is normally abbreviated as MLE (Maximum Likelihood Estimate):

$$\widehat{\theta}_{ML} = MLE = \max_{\theta} \ p(Y|\theta) \tag{43}$$

In practice maximizing the likelihood is equivalent to maximizing the log-likelihood function $L_{log} = log(p(Y|\theta))$, which is the same as minimizing $-log(p(Y|\theta))$. This results in the following target function:

$$-L_{log} = -log(p(Y|\theta)) = \sum_{i=1}^{n} 0.5\sigma^{-2}(Y_i - f(X_i, \theta))^2 + 0.5n\log(2\pi\sigma^2) \tag{44}$$

This kind of objective function is often chosen, because it is easier to optimize than the likelihood itself. Also some optimization routines are especially designed for objective functions that contains sums of squares. In addition, the optimization routines often assume that the objective function is to be minimized and that is why the minus sign is used.

6.2 Monte Carlo Methods

The term *Monte Carlo*(MC) methods is normally expressed in a very general way. MC methods are stochastic methods; methods that involve sampling random numbers from probability distributions to investigate a certain problem. The Monte Carlo methods are mainly maint for solving two kinds of problems that often arise in statistical analysis. MC methods provide a way to generate samples from a given probability distribution. On the other hand they give a solution to the problem of estimating expectations of functions under some distribution and thus calculating numerical approximations for integrals.

A major issue in statistics is the ability to create samples from a given probability distribution. In the Bayesian framework, we want to create samples from the posterior density in order to examine the correlation and accuracy of model parameters and predictions. The Monte Carlo based methods rely on the possibility of creating random variables from arbitrary and possibly complex distributions. There are different methodology of sampling from different distributions and the detailed description of these methods can be found in [25].

6.3 Markov Chain Monte Carlo Methods

In Bayesian analysis for unknown parameters we are often interested in forming the posterior distribution for the parameters. Since this is rarelly possible to do analytically, we are satisfied with a number of samples from the posterior distribution of the model parameters. To achieve this by applying the Bayes' rule given by the Equation 35 one has to integrate over the whole parameter space to calculate the normalizing constant for the posterior density. A numerical approximation can be achieved through Monte Carlo integration [25]. Especially in high dimensional cases, however, these methods might be problematic. But with MCMC methods, the posterior distribution can be evaluated without having to worry about the problematic normalizing constant of the Bayes' rule.

The main idea behind MCMC methods is to create a certain type of Markov Chain that represents the posterior distribution. For more detailed description related to the basics about stochastic processes and Markov Chains, refer to [28].

A Markov Process is a certain type of discrete time stochatic process. A Markov Chain is a series of states created by a Markov Process. Assume that we have a series of random

variables, $(X^{(0)}, X^{(1)}, X^{(2)}, \ldots)$. This series is a Markov Chain, if the value of $X^{(t+1)}$ only depends on the value of the previous state $X^{(t)}$. Formally,

$$P(X^{(t+1)} = s_{t+1} | X^{(0)} = s_0, X^{(1)} = s_1, \ldots, X^{(t)} = s_t) = P(X^{(t+1)} = s_{t+1} | X^{(t)} = s_t) \tag{45}$$

where s_i denotes the state of the chain at time i.

In MCMC methods the idea is to create a Markov Chain using random sampling so that the created chain has the posterior distribution as its unique stationary distribution (limiting distribution). The most basic methods of achieving this, the Metropolis algorithm and its generalization (Metropolis-Hastings algorithm) are introduced in the following section.

6.3.1 Metropolis-Hastings Algorithm

The Metropolis-Hastings (MH) algorithm prescribes a simple transition kernel to produce a Markov Chain that has invariant distribution $\pi(\theta)$ that can be regarded as a sample from $\pi(\theta)$. The MH algorithm is based on accept-reject methodology: a new candidate point θ^* is created from a proposal distribution $q(.|\theta)$ that contains the probabilities for recieving a certain candidate point given the previous value θ. The MH algorithm can be written as follows [25]:

1. Initialization

   - Choose a starting point θ_0
   - Set $\theta_{old} = \theta_0$
   - Set $Chain(1) = \theta_0$ and $i = 2$

   Choose a new candidate from the proposal distribution: $\theta^* \sim q(.|\theta_{old})$

2. Accept the candidate with probability

$$\alpha = \min \left(1, \frac{\pi(\theta^*) q(\theta_{old}|\theta^*)}{\pi(\theta_{old}) q(\theta^*|\theta_{old})}\right) \tag{46}$$

   - If accepted set $Chain(i) = \theta^*$ and $\theta_{old} = \theta^*$

- If rejected set $Chain(i) = \theta_{old}$

3. Set $i = i + 1$ and go to 2.

If we assume a symmetric proposal distribution, that is, $q(\theta^*|\theta_{old}) = q(\theta_{old}|\theta^*)$, we get a special case of the MH algorithm called the Metropolis algorithm.

Note here that if we use the Bayesian framework we know the posterior density up to a normalizing constant. We see that in Equation 46 the constant cancels out. If we assume a standard nonlinear model ($Y = f(X, \theta)$) with Gaussian noise ($\epsilon \sim N(0, \sigma^2 I)$) and a non-informative prior $\pi_{pr}(\theta) = 1$, we can write the acceptance probability for the Metropolis algorithm as follows:

$$\alpha = \min\left(1, \frac{\pi(\theta^*)}{\pi(\theta_{old})}\right) = \min\left(1, \frac{p(Y|\theta^*)}{p(Y|\theta_{old})}\right) = \min\left(1, e^{-0.5\sigma^{-2}(SS_{\theta^*} - SS_{\theta_{old}})}\right) \quad (47)$$

This is a practical form of the acceptance rule and is the basis of the implementation of MCMC methods in any statistical analysis case. The third step (acceptance step) of the algorithm can now be written in a more practical way as follows:
3. Compute SS_{θ^*} and $SS_{\theta_{old}}$. Accept the candidate if $SS_{\theta^*} < SS_{\theta_{old}}$ or if $u < e^{-0.5\sigma^{-2}(SS_{\theta^*} - SS_{\theta_{old}})}$ where u is a random number generated from $U[0, 1]$.

6.3.2 MCMC Sampling and how the Chain is used Inside the Optimizer

Let us return to the heat recovery model, during the MCMC sampling, the Nusselt numbers described in Equation 5 are expressed in a new parametrized form to present the uncertainty of the Nusselt numbers for both exhaust and supply fluid side of the heat recovery unit and is written as follows:

$$Nu_{exh} = \theta_1 Re^{\theta_2} Pr^{\theta_3} \quad (48)$$

$$Nu_{supp} = \theta_1 Re^{\theta_2} Pr^{\theta_4} \quad (49)$$

respectively. From the Equations 48 and 49 the first two parameters for both exhaust and supply fluid side are the same, only θ_3 and θ_4 are different.

The author [11] defines the general $cmnn-$ model as

$$Y = f(X, \theta) + \epsilon \tag{50}$$

where $\{\theta = \theta_1, \theta_2, \theta_3, \theta_4\}$ contains the c, m, n, n parameters, and Y is the $cmnn-$model response, and X contains the synthetical data made from c, m, n, n constant values, and ϵ is the noise level used to create the synthetical data. The prior knowledge of θ parameters used in the sampling was assumed to be uniformly distributed, and the chains were collected after 20000 simulations.

During the optimization of the dry heat exchanger sub-process, several cost functions are optimized at the same time. Both outgoing exhaust and supply fluid temperatures ($T_{exh,out}$ and $T_{supp,out}$) depend on the incoming fluid properties and control variables of the dry heat exchanger unit whereas the heat recovered energy (Φ_{HR}) depends on both incoming and outgoing fluid properties and control variables. This inter-dependence of the parameters makes the system behaving nonlinearly. For that reason, MCMC methods are used at this stage to take into consideration the uncertainty in the created models.

Consider a general optimization equation below:

$$\min f(d_{exh}, d_{supp}, L, H, N) \tag{51}$$

subject to

$$\text{L.B} \leq d_{exh}, d_{supp}, L, H, N \leq U.B$$

and compute

$$\begin{gathered} \mathrm{T}^i_{supp,out} = f(X_{in}, \theta_i, L, H, N) \\ \mathrm{T}^i_{exh,out} = f(X_{in}, \theta_i, L, H, N) \\ \Phi^i_{HR} = f(X_{in}, \theta_i, d_{exh}, d_{supp}, L, H, N, T_{supp,out}, T_{exh,out}) \end{gathered}$$

The $L.B$ and $U.B$ are the lower and upper bounds for the given control variables. $\{\theta_i, i = 1, .., j\}$ are the parameter chains from the Nusselt number for both exhaust and supply fluid, and

X_{in} contains the incoming fluid flow variables such as the incoming exhaust and supply fluid temperatures and their corresponding mass flow, the amount of humid air, etc.

The question is to find out an effective way to use these parameter chains inside the optimizer to get the distributions of the optimal solution. This question can be solved in different ways in which three approaches are described as follows:

Approach 1

This approach is applied by fixing the parameter chain (θ_i) for the heat exchanger model during the optimization process. This means that the mean value of the chain is given inside the optimizer during the cost function evaluations, and the calculation of the predictions of outgoing temperatures and the heat recovered energy is performed by accepting only solutions which satisfy all the constraints given in Equation 51.

Approach 2

Approach 2 is mainly based on the constraints to be considered in the optimization models. In general all the points from the chain (θ_i) should be given inside the optimizer during the cost function evaluations, and the optimization is done so that all the constraints are taken into account at the same time, this means that the optimization is done many times depending on the number of constraints. Due to the CPU time waiting, different random selected points from the chain are given inside the optimizer instead of the whole chain (θ_i). The optimization algorithm has to be run long enough to ensure its convergence.

Approach 3

In general, all the chain points (θ_i) are given inside the optimizer during the cost function evaluations. This means that the optimization is done many times depending on the number of the chain points. In other words, the optimization is done for every given point from the chain (θ_i), and different optimal solutions from different optimization runs based on different points from the chain have to be saved. However, since the CPU waiting time in this case is very long different points from the chain have to be selected randomly to present the sample, and the population size and generation number have to be bigger

enough to ensure the convergence of the algorithm.

7 Implementation Methodology of the Case Study

Functional principle of the model is presented in Figure 1 which describles the connections between the heat recovery units. Mathematical approach and parameters for these unit processes are presented in the previous sections. To generate the sufficient solver for the optimization the development environment has to have reasonable function libraries and solvers to handle the presented nonlinear problems and also to combine optimization and simulation. Several programming environments include needed features for the model implementation. The project work involves several objective functions to be optimized at the same time, and this leads to the choice of NSGA-II as one of the multiobjective optimization methods to be used. This algorithm is implemented in Matlab environment and it is described as a package of several Matlab files.

Due to the number of control variables and several sub-models the non-linearity rules the system character. For that reason, it can be assumed that the solution domain includes several local minimums and maximums, and due to this it is important to evaluate the whole problem field and be sure that the achieved results represent a global optimum. The plan is to start the optimization with NSGA-II to seek the domain for the control variables giving the optimal solution. After the control variables have reached the range where the values are not any more varying over the given limits the optimization method will be used to optimize the created cost functions at the same time. After the optimization step, the MCMC methods will be used inside the optimizer as described in section 6.3.2 for taking into account account the uncertainty in the optimization models.

7.1 Structure of the Heat Recovery Units used in the Case Study

7.1.1 Dry Heat Recovery Unit

As mentioned earlier the dry heat recovery (DHR) unit is composed of several plates separated by empty space called *duct* whose size is called *slot size*. All the slots on the supply air side have the same slot size and all the slots on the exhaust air side have the same slot size. However, the slot sizes for both exhaust and supply air side of the unit do

not have to be the same.

The measured parameter for DHR unit on supply air direction is the plate size denoted by *L*, and on exhaust air direction the measured parameter is the plate size denoted by *H*, and the third parameter is the width *W* of the whole unit given by the sum of all slot widths inside the unit. The dry heat recovery unit considered in this case study has the following measured standard parameter values:

$$d_{exh} \in (0.016, 0.020)\ \text{m}$$
$$d_{supp} \in (0.016, 0.020)\ \text{m}$$
$$L_{DHR} \in (2, 2.5, 3)\ \text{m}$$
$$H_{DHR} \in (1, 1.25)\ \text{m}$$
$$N_{DHR} \in (40, 150)$$

These limitations are due to the engineering practical point of view that the manifacturers can only produce the plate heat exchangers based on these standard parameter values.

7.1.2 Wet Heat Recovery Unit

The wet heat recovery (WHR) unit described in Figure 4 has the following standard parameter values:

$$d_{exh} = 0.011\ \text{m}$$
$$d_{supp} = 0.004\ \text{m}$$
$$L_{WHR} \in (1.8, 2, 2.2)\ \text{m}$$
$$H_{DHR} \in (1, 1.25)\ \text{m}$$
$$N_{DHR} \in (14, 200)$$

7.2 Model Calculation and Control Variable Selection

The model presented in the previous sections is divided into the sub-process connected together with process connections. In this case study these connections are dry and wet heat recovery units having the supply and exhaust fluids inside. The calculation synthax of the model follows the direction of the supply and exhaust fluids starting from heat

recovery units, which are the base element for the system. By means of modeling both dry and wet heat recovery units need back calculations inside the model due to counter-current cross flow and phase changes. When the physical setup of the system is created the objective function for LCC is formulated and the related factors are calculated as follows:

$$LCC = \sum_{t=0}^{t_{lifespan}} \frac{1}{(1+r)^t} I_t + a_e^{''} E_{el} + a_h^{''} e_h E_h \tag{52}$$

where

$$E_{el} = E_{el,exh} + E_{el,supp} \tag{53}$$

$$E_{el,exh} = \eta_p^{-1} \eta_l e_e K V_{exh} \Delta P_{exh} \tag{54}$$

$$E_{el,supp} = \eta_p^{-1} \eta_l e_e K V_{supp} \Delta P_{supp} \tag{55}$$

and

E_{el}	total electric power consumed by the pump machine	[kWh]
$E_{el,exh}$	electric power used by the pump machine on exhaust fluid side	[kWh]
$E_{el,supp}$	electric power used by the pump machine on supply fluid side	[kWh]
η_p	efficiency of the pump machine	[%]
η_l	loss coefficient associated to the pump machine	[-]
K	operating time	[hours/a]
V_{supp}	volumetric flow rate of the supply fluid	[m^3/s]
V_{exh}	volumetric flow rate of the exhaust fluid	[m^3/s]
ΔP_{exh}	pressure drop on the exhaust fluid side	[Pa]
ΔP_{supp}	pressure drop on the supply fluid side	[Pa]

It is assumed that the pump / fan machines have the same efficiency, the same loss coefficient and the same operating time through the whole system.

This LCC function includes the investment terms which are the price of the heat recovery units of the system themselves and the total cost for heating units. The LCC function includes also the operating cost terms which are the cost of additional steam energy needed when the energy produced by the heat recovery units is not enough for the heating demand, and the cost for electricity consumed by the pump / fan machines [29].

The annual energy consumption for heating the supply air or for heating the supply water in heat exchanger system is calculated as follows:

$$E_h = q_{m,supp} c_p \left(T_{final} - T_{supp,i}\right) \tag{56}$$

where

T_{final}	desired final temperature value	[^{o}C]
$T_{supp,i}$	incoming supply fluid temperature	[^{o}C]

In general T_{final} can be assumed to be constant around the year, and in this case study, the final temperature to which the supply air has to be heated is fixed to 100^o C, while the final temperature to which the supply water has to be heated is fixed to 55^oC.

Since the investment terms are directly related to the total area of the heat recovery units, the given optimization function in Equation 52 has to be minimized at the same time with the following cost function for minimizing the area of the whole system.

$$\min A_{HR} \tag{57}$$

subject to

$$L_{DHR} \in (2, 2.5, 3)\text{m}$$
$$H_{DHR} \in (1, 1.25)\text{m}$$
$$N_{DHR} \in (40, 150)$$
$$L_{WHR} \in (1.8, 2, 2.2)\text{m}$$
$$H_{WHR} \in (1, 1.25)\text{m}$$
$$N_{WHR} \in (14, 200)$$

where

$$A_{HR} = A_{DHR} + A_{WHR}$$
$$A_{DHR} = 2(N_{DHR} - 1) L_{DHR} H_{DHR}$$
$$A_{WHR} = 2(N_{WHR} - 1) L_{WHR} H_{WHR}$$

During the implementation the following practical assumptions and facts were observed:

1. The outgoing temperature of the supply air ($T_{supp,air,out}$) was changing with respect

to different geometry of the heat recovery unit. In practice, This outgoing temperature has to be considered as a control variable during the optimization process.

2. $T_{supp,water,out} < T_{dp}$. If the supply water is heated to higher temperature than exhaust air dew point temperature the heat exchanger size will be increased remarkably. Another remarkable reason for this limitation was that heat exchanger model became often unstable when heat surfaces were partly dry. This constraint has been also taken into account during the optimization.

3. The mass flow of supply water ($q_{m,supp,water}$) has a remarkable effect on the system. In practice, the slot size on the supply water side is relatively small if the water flow going inside the heat exchanger is much enough the whole system could be destroyed. This parameter has been taken into account as a control variable and let the optimizer finds the optimal value depending on the optimal geometry of the heat recovery unit.

During the optimization process, the velocity of the fluid inside the heat exchanger has to be taken into account as well. In practice, the velocity inside the heat exchanger varies between $8 - 12$ m/s and sometimes it goes up to 15 m/s. We have to let the fluid flow going inside the heat exchanger to be within acceptable ranges, and be penalized if the velocity is approaching 15 m/s or if it is going below 8 m/s. The fluid velocity inside the heat exchanger going beyond 15 m/s has to be rejected. This constraint is implemented as a penality function described in Figure 10 .

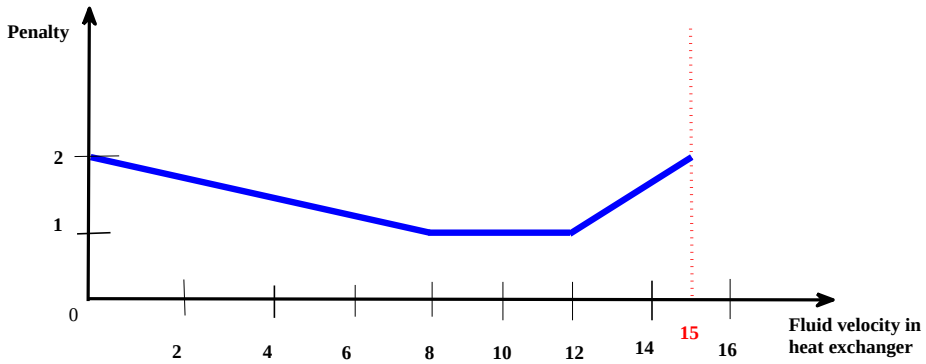

Figure 10: Penalty function for fluid velocity inside the heat exchanger

The penalty function used in this case is defined as follows:

$$P(w) = \begin{cases} \frac{1}{3}w - \frac{5}{2} & \text{if } 12 < w \leq 15 \\ 1 & \text{if } 8 \leq w \leq 12 \\ \frac{-1}{8}w + 2 & \text{if } w < 8 \end{cases}$$

where w is the fluid velocity inside the heat exchanger. This penalty function affects only the investment terms through the cost of the heat recovery units. For that reason, the cost of heat recovery units themselves will be penalized as follows:

$$Cost_{HR} = P_{exh} \times P_{supp} \times A_{HR} \times Ca \tag{58}$$

where

$Cost_{HR}$	cost of heat recovery unit	[EUR]
P_{exh}	penalty term on the exhaust fluid side	[-]
P_{supp}	penalty term on the supply fluid side	[-]
A_{HR}	area of heat recovery unit	[m^2]
Ca	price of surface unit	[EUR/m^2]

8 Results

To analyze the created simulation and optimization models they were tested against the industrial project considered as a case study in this Master's thesis.

8.1 Optimization Results

Optimization of the design values was done with different test runs. Parametrization of the models are presented in Table 3 and the differences between the test run alternatives are shown in Table 1 while the specific parameters given in Table 2 are used in all optimization cases. That is, the specific parameters are always the same in all three different life cycle periods of the case study project.

Table 1: Optimization cases.

Parameter	Run 1	Run 2	Run 3
Life cycle period	5 a	10 a	15 a

Table 2: Specific parametrization of the optimization cases.

Parameter	Value
Escalation of electrical energy (e_e)	5 %
Escalation of heat energy (e_h)	5 %
Inflation rate	2 %
Nominal interest rate	7 %
Efficiency of the pump	75 %
Incoming exhaust air temperature	$+80^o$ C
Incoming supply air temperature	$+28^o$ C
Incoming supply water temperature	$+10^o$ C
Incoming exhaust air mass flow	30 kg/s
Incoming supply air mass flow	20 kg/s
Incoming exhaust air water content	160 gH_2O/kg
Incoming supply air water content	20 gH_2O/kg
Operating time	8400 hours/a
Price of dry heat recovery unit	50 EUR/m^2
Price of wet heat recovery unit	160 EUR/m^2
Price for heating unit (dry heat recovery)	12 EUR/kW
Price of steam energy	30 EUR/MWh
Price of electricity	60 EUR/MWh

The cost for heating water in a wet heat recovery unit is estimated by the following equation:

$$C_{coil} = 5000 + 5E_h \tag{59}$$

where E_h is the annual energy consumption for water heating and it can be calculated by the Equation 56, and the constant values 5000 and 5 are the Euros.

The control variable limits were chosen based on the above described unit process properties. Size of the population was chosen to be at least two times compared to the number of control variables. The number of generations was fixed after the preliminary tests of the model together with the NSGA-II toolbox.

Table 3: Parametrization of the optimization algorithm.

Control variable	Lower limit	Upper limit
Outgoing supply air temperature	50^o C	60^o C
Incoming supply water mass flow	10 kg/s	30 kg/s
Slot size on the exhaust air side	0.016 m	0.020 m
Slot size on the supply air side	0.016 m	0.020 m
Plate size on the supply air side (dry heat recovery)	2 m	3 m
Plate size on the exhaust air side	1 m	1.25 m
Plate size on the supply air side (wet heat recovery)	1.8 m	2.2 m
Number of slots inside dry heat recovery unit	40	150
Number of slots inside wet heat recovery unit	14	200
Size of the population	500	-
Number of generations	1000	-

8.1.1 Results from the Dry Heat Exchanger Sub-process

After tuning NSGA-II toolbox the optimization runs were done for the cases shown in Table 1. During the optimization of LCC function which represents the price of the saved energy, it was found that the price of the recovered energy is 43.13 EUR/MWh which is feasible to heat the supply air up to 59^o C. The optimal design for a dry heat recovery unit is shown in Table 4.

Table 4: Optimal design parameter values for the dry heat exchanger.

Parameter	Value
Slot size on the exhaust air side	0.0161 m
Slot size on the supply air side	0.0162 m
Plate size on the supply air side	3 m
Plate side on the exhaust air side	1 m
Number of the slots inside heat exchanger	66
Outgoing supply air temperature	59^o C
Area of a heat exchanger unit	390 m^2
Heat recovered from the dry heat exchanger	676.2 kW

The visualization of the optimization was done by plotting CAPEX vs. Annual OPEX where the CAPEX is the sum of the costs of heat recovery unit and the costs for heating units, while the OPEX is the sum of the costs of steam heating and the costs of electrical energy consumed by the pump. The results for the cases are presented in Figure 11 and Figure 12.

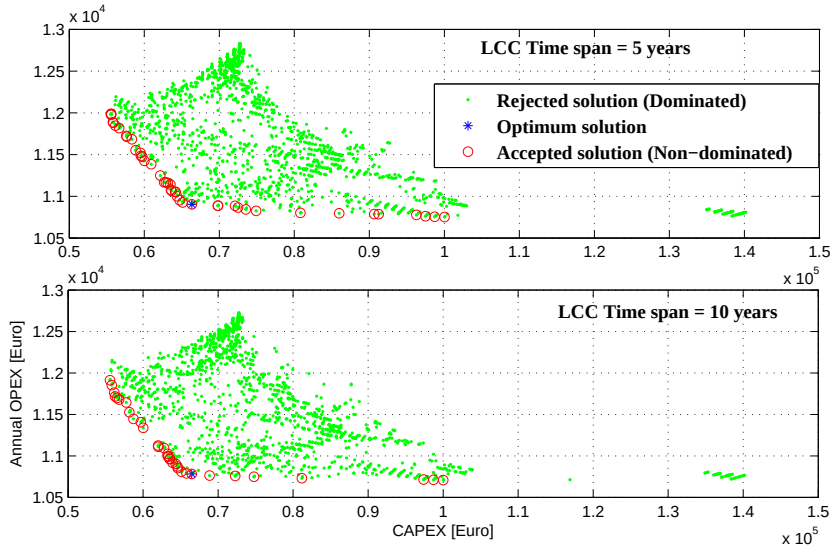

Figure 11: Pareto front of CAPEX vs. Annual OPEX for 5 and 10 years life span.

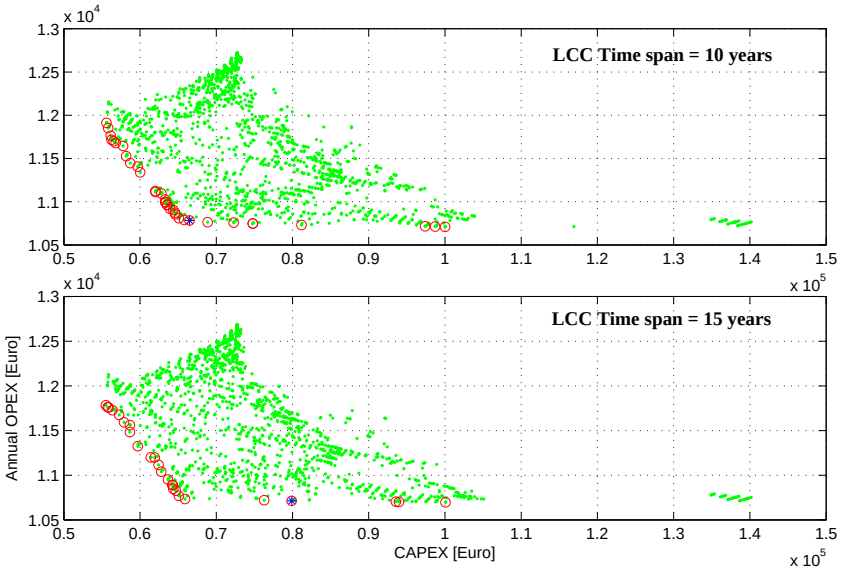

Figure 12: Pareto front of CAPEX vs. Annual OPEX for 10 and 15 years life span.

From the result figures can be seen that the model is responding as expected. The longer lifetime weights higher CAPEX and lower OPEX and vice versa. Pareto front for the cases are shown on red cycled points in the figures. Table 5 shows this behavior of the investment.

Table 5: Behavior of the investment in dry heat exchanger.

Project life span	CAPEX	Annual OPEX
5 years	63553 Euros	11077 Euros
10 years	65784 Euros	10789 Euros
15 years	79878 Euros	10712 Euros

8.1.2 Results from the Whole System

In this case, dry and wet heat recovery units are combined together and the optimization of the LCC function of the whole system is done together with optimizing the design of the system at the same time. The optimal price of the saved energy for the system is 58.18 EUR/MWh which is feasible for heating the supply air up to 59^o C and for heating the supply water up to 58^o C at the same time. The optimization design results of the system are shown in Table 6.

Table 6: Optimal design parameter values for the whole system.

Parameter	Value
Slot size on the exhaust air side	0.020 m
Slot size on the supply air side	0.0192 m
Plate size on the supply air side	2 m
Plate size on the exhaust air side	1 m
Number of the slots inside a dry heat exchanger	80
Outgoing supply air temperature	59^o C
Area of a dry heat exchanger unit	316 m^2
Heat recovered from the dry heat exchanger	518.8 kW
Plate size on the supply water side	2.2 m
Plate size on the exhaust air side of the wet heat exchanger	1 m
Number of slots inside a wet heat exchanger	27
Incoming supply water mass flow	21 kg/s
Outgoing supply water temperature	58^o C
Area of a wet heat exchanger unit	114 m^2
Heat recovered from the wet heat exchanger	3182.8 kW

Table 6 shows that the optimal supply water mass flow is 21 kg/s which requires a corresponding wet heat exchanger area of 114 m^2 compared to a dry heat exchanger area 316 m^2 in order that supply water temperature $+10^o$ C is to be heated at a final temperature 55^o C without exceeding the dew point temperature 61.05^o C calculated by [11] during the simulation process.

From the Table 6 one can see that the wet heat exchanger is much more efficient than the dry heat exchanger by comparing the heat recovered from two different heat recovery units and the corresponding required surface area. These results show that the dry heat exchanger requires 316 m^2 of surface area for recovering only 518.8 kW, while the wet heat exchanger requires 114 m^2 of surface area to recover 3182.8 kW. In terms of ratios, one can gain around 28 kW/m^2 from the wet heat recovery unit, while in the dry heat exchanger the heat recovered per m^2 is only around 1.64 kW/m^2. Even though it is expensive to construct a wet heat exchanger compared to the construction of a dry heat exchanger as shown in Table 2 it can be beneficial to use only a small wet heat exchanger than implementing big dry heat exchanger with which one can gain less recovered energy.

The visualization of the optimization results for the whole system was done by plotting CAPEX vs. Annual OPEX as usual. The results for different cases are presented in Figure 13 and Figure 14.

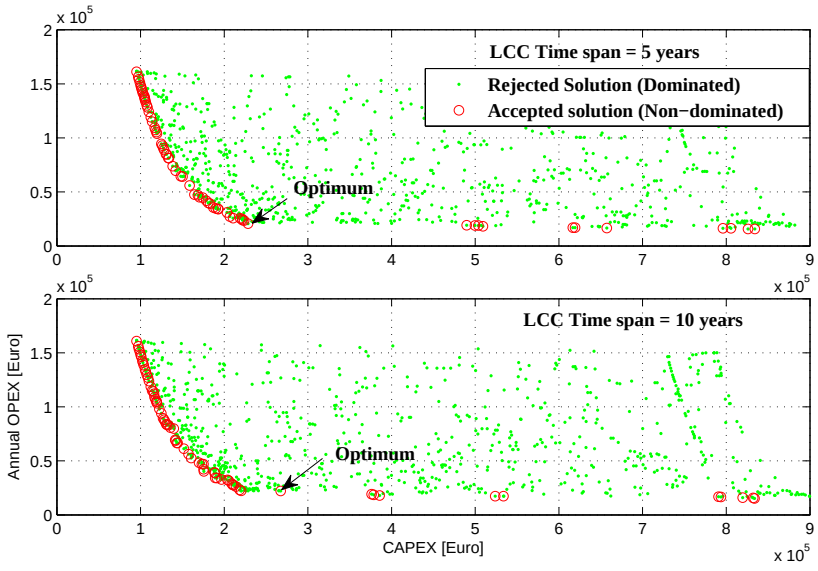

Figure 13: Pareto front of CAPEX vs. Annual OPEX for 5 and 10 years for the whole system.

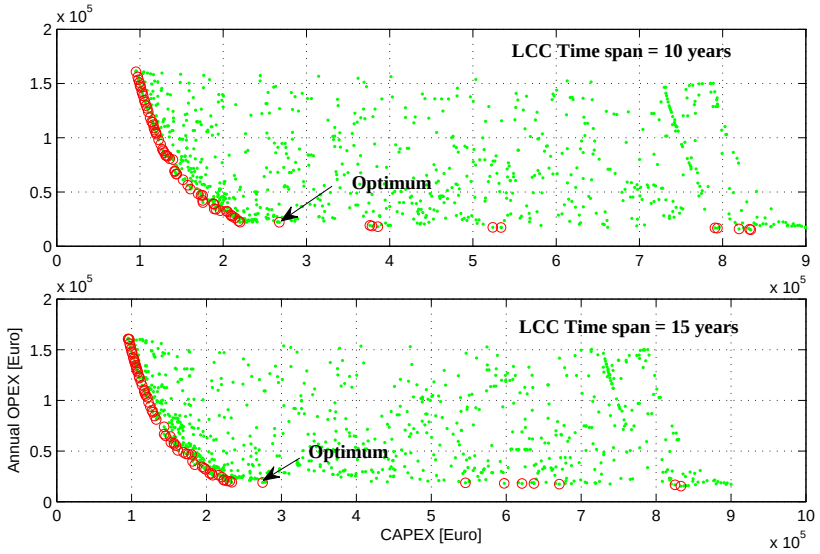

Figure 14: Pareto front of CAPEX vs. Annual OPEX for 10 and 15 years for the whole system.

As in the dry heat exchanger case, the same behavior of investment is realized in the whole system. The longer lifetime weights higher CAPEX and lower OPEX and vice versa. This behavior is also shown in Table 7.

Table 7: Behavior of the investment for the whole system.

Project life span	CAPEX	Annual OPEX
5 years	228360 Euros	22090 Euros
10 years	267410 Euros	21610 Euros
15 years	274890 Euros	18870 Euros

The results so far indicate that dry heat exchangers are less efficient and they usually require bigger operating surface area with relative small recovered energy compared to wet heat exchangers.

8.2 Results from the MCMC Methods for the Dry Heat Exchanger Sub-process

During the implementation of MCMC methods on the top of optimization algorithm (NSGA-II), a simplified case of minimizing the area of a dry heat exchanger was used.

For the understanding of how the proposed approaches are working, the slot size on both exhaust and supply air side d_{exh} and d_{supp} respectively, and the number of slots N_{DHR} inside the heat exchanger were fixed to the values given below. Therefore, the cost function to be minimized is defined as follows:

$$\min A_{HR} \tag{60}$$

subject to

$$L_{DHR} \in (2, 3)\ \text{m}$$
$$H_{DHR} \in (1, 2)\ \text{m}$$
$$N_{DHR} = 80$$
$$d_{exh} = 0.016\ \text{m}$$
$$d_{supp} = 0.016\ \text{m}$$

where

$$A_{HR} = 2(N_{DHR} - 1)L_{DHR}H_{DHR}$$

The usual optimization is done first by fixing the parameter chain during the optimization process, i.e. the mean value of the chain is given inside the optimizer during the cost function evaluations and long run (population size of 40 and generation number of 1000) of the optimization algorithm is performed. After the population members have converged to the optimum, the optimal solution of the last generation is presented in Figure 15.

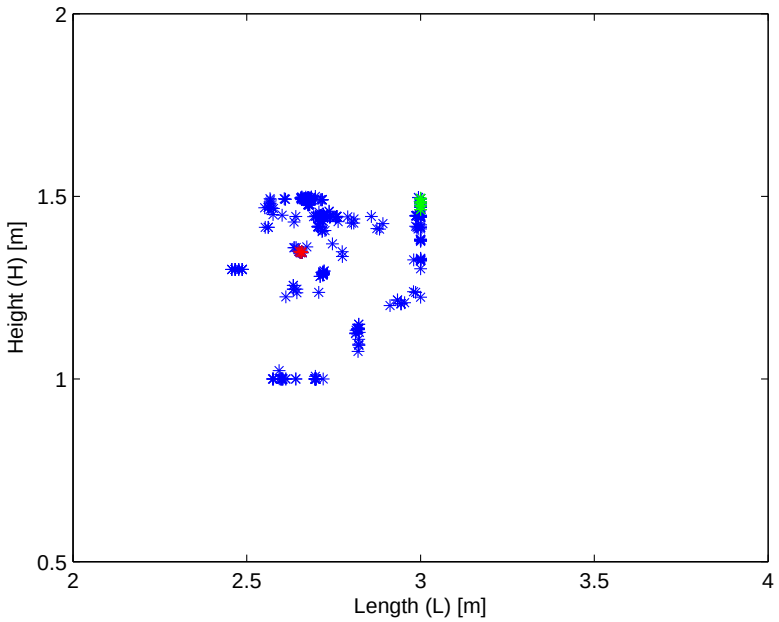

Figure 15: Optimal solutions (Red: for the mean value of the chain, Green: for all constraints, Blue: for some points from the chain).

Figure 15 in red points shows that the implementation of approach 1 described in section 6.3.2 results in a small heat exchanger whose optimal slot size on the supply air direction L is 2.65 m^2, while the slot size on the exhaust air direction is H is 1.34 m^2. And it is well seen that all the population members of the last generation have converged to the optimum.

The implementation of approach 2 in which the optimization is done by going through all the given constraints corresponding to different points from the chain results in a little bit bigger heat exchanger as shown in Figure 15 in green points. One can see that the optimal slot size on the exhaut air side H was increased up to 1.5 m^2 while the optimal slot size on the supply air side L is also increased up to 3 m^2.

The implementation of approach 3 in which the optimization is done several times depending on the points from the chain results in different optimal solutions from different optimization runs as shown in Figure 15 in blue points. In this case all the population members from the last generation of every optimization run which corresponds to the random selected points from the chain θ_i have converged to different optimal solutions. One can see that for each point from the chain the algorithm results in a different optimal design. This clearly shows how much the uncertainty in the models can affect the results from the usual optimization.

In Figure 15 in blue points all the optimal solutions from different optimization runs based on different points from the chain are varying around the optimal solution obtained by using the mean value from the chain (red points) and the optimal solutions obtained from the implementation of approach 2 (green points). With these results the safe limits in which the decision makers can choose the optimal design of a dry heat exchanger are clearly known, and with these results different dry heat exchangers can be designed with a 95 % of confidence.

8.3 Discussion and Future Work

The NSGA-II algorithm is working as expected but is slow for the whole system, since it requires the evaluation of a large population size and a large number of generations which leads to big CPU time waiting in practical engineering cases. Three different approaches of implementing the MCMC methods inside the optimizer have been implemented succesfully by using a simplified case of minimizing the area of a dry heat exchanger. One can think on improving the running CPU time and the implementation of MCMC methods inside the optimizer for complex optimization models.

There are three main things which can be taken into consideration. One way is to parallelize NSGA-II algorithm in such way that at each generation all N population can be evaluated independently on different processors, since the central algorithm only needs the values of the objectives to iterate. This parallelization can be implemented using the C interfacing program responsible for the evaluation of the objective function values associated with N population.

The second possibility is to use Kalman Filter methods which explicitly specify the uncertainty in the system states that arises from imperfect process approximation and from data uncertainty. In this way, one might calculate the outgoing exhaust and supply fluid temperature predictions from the dry heat exchanger to be the incoming fluid temperature of the following wet heat exchanger. Since both outgoing exhaust and supply fluid temperature are used to connect different types of heat exchangers, with these methods, one might be able to take into consideration the uncertainty in the models of the whole system.

The third possibility is to apply the described approaches for implementing the MCMC methods inside the optimizer to the complex optimization methods (the whole system),

by first of all checking if the chain remains completely the same for different geometry of a heat exchanger. If the chain remains the same for different geometry parameters of a heat exchanger then the described approaches of implementing MCMC methods inside the optimizer will be used as they are by letting all the control variables varying within the given ranges. If the chain is different for different geometry parameters, then the described approaches have to be modified appropriately.

9 Conclusions

Presented optimization and statistical analysis work included the optimization models for the heat exchanger network including heat recovery. Implementation of the models was done in Matlab environment in which the design optimization was done by utilizing a Nondominated Sorting Genetic Algorithm II (NSGA-II), while the statistical analysis was done by using the Markov Chain Monte Carlo(MCMC) methods.

The optimization models for dimensioning the plate heat exchanger network that satisfy the goals set for creating and minimizing the LCC function which represents the price of the saved energy, for minimizing the whole system network area and for maximizing the momentary heat recovery outputs were successfully formulated. The uncertainty in the model for the simplified case (dry heat exchanger sub-process) was taken into account during the optimization process and the results were promising.

The design optimization of a dry heat exchanger sub-process results in an area of 390 m^2 with a heat recovered of only 676.2 kWh. The minimization of the LCC function in this case has shown that the optimal price of saved energy 43.13 EUR/MWh is feasible for heating the supply air up to 59^o C.

During the optimization process of the whole system, i.e. when a dry and a wet heat exchangers are combined together the LCC function was minimized together with minimizing the area of the system and miximizing the momentary heat recovery output. The optimal price of saved energy for the system was found to be 58.18 EUR/MWh which is feasible for heating the supply air temperature 28^o C to a temperature 59^o C and for heating the supply water temperature $+10^o$ C to a temperature 58^o C at the same time. The design optimization results of the system have shown that the wet heat exchangers are more efficient compared to dry heat exchangers since the wet heat exchanger unit requires an operating surface area of 114 m^2 to recover the heat of 3182.8 kWh, while

a dry heat exchanger requires an operating surface area of 316 m ^{2} for recovering only 518.8 kWh. This was an indication that even though it is expensive to construct a wet heat exchanger (160 EUR/m^2) compared to the construction of a dry heat exchanger (50 EUR/m^2) it can be beneficial to use only a small wet heat exchanger than implementing a big dry heat exchanger with which one can gain less recovered energy.

The investment behavior of the project was studied by analyzing the CAPEX and OPEX based on the avalaible factors which affect the investment costs and operating costs for both cases (dry heat exchanger sub-process and combined dry and wet heat exchangers). The CAPEX and OPEX results have shown that the created optimization models were responding as expected. The longer lifetime weights higher CAPEX and lower OPEX and vice versa. That is, it is cheaper to invest for short period but the operating costs will be higher annually.

When the uncertainty in the models was taken into account during the optimization process by implementing three different described approaches, it has been found that for each point from the chain the algorithm results in a different optimal design. This clearly shows how much the uncertainty in the models can affect the results from the usual optimization. All the optimal solutions from different optimization runs based on different points from the chain were varying between the optimal solutions obtained from the implementation of both approach 1 and approach 2. With these results the safe limits in which the decision makers can choose the optimal design of a dry heat exchanger were clearly known, and with these results different dry heat exchangers can be designed with a 95 % of confidence.

References

[1] Frank P. Incropera and David P. Dewitt and Theodore L. Bergman and Adrienne S. Lavine. *Fundamentals of Heat and Mass Transfer*, Sixth Edition, John Wiley Sons,Inc., United States of America, 2007, ISBN: 0-471-38650-2

[2] Philippe Wildi-Tremblay and Louis Gosselin. *Minimizing shell and tube heat exchanger cost with genetic algorithms and considering maintenance,* International Journal of Energy Research, Vol 31, pages 867-885, November 2006

[3] Jose M.Ponce-Ortega and Medardo Serna-Gonzalez and Arturo Jimenez-Gutierrez. *Heat exchanger network synthesis including detailed heat exchanger design using genetic algorithms,* Ind.Eng.Chem, Vol 46, pages 8767-8780, September 2007

[4] A. Unuvar and S. Kargici. *An approach for the optimum design of heat exchangers*, Internatioanl Journal of Energy Research, Vol 28, pages 1379-1392, January 2004

[5] S. Frausto-Hernandez and V. Rico-Ramirez and A. Jimenez-Gutierrez. *MINLP synthesis of heat exchanger networks considering pressure drop effects,* Computers Chemical Engineering, Vol 27, pages 1143-1152, February 2003

[6] Renan Hilbert and Gabor Janiga and Romain Baron and Dominique Thevenin. *Multi-objective shape optimization of a heat exchanger using parallel genetic algorithms,* Heat and Mass Transfer, Vol 49, pages 2567-2577, March 2006

[7] Alireza Nazemi and Xin Yao and Andrew H. Chan. *Extracting a set of robust Pareto-optimal parameters for hydrologic models using NSGA-II and SCEM*, IEEE Congress on Evolutionary Computation, Vancouver, BC, Canada, July 16-21 2006

[8] Leena Kilponen. *Improvement of heat recovery in existing paper machines*, Licentiate thesis, Helsinki University of Technology, Espoo, November 2002

[9] Jung-Yang San, and Chin-Lon Jan. *Second law of a wet crossflow heat exchanger*, Energy, Vol 25, pages 939-955, 2000

[10] Mauri Soininen. *Dimensioning of Paper Machine Heat Recovery Recuperators*, Drying Technology, Vol 13, pages 867-896, 1995

[11] Taavi Aalto. *Statistical Analyis and Numerics of Heat Exchanger Models*, Master's thesis, Lappeenranta University of Technology, Lappeenranta, to appear in 2009

[12] Frank M. White. *Fluid Mechanics,* Fourth Edition, The McGraw-Hill Companies, Inc., Singapore, 1999, ISBN: 0-07-116848-6

[13] Randy L. Haupt, and Sue Ellen Haupt. *Practical Genetic Algorithms*, John Wiley Sons Inc., A Wiley-Interscience publication, U.S.A, 1998, ISBN: 0-471-18873-5

[14] Essi Välimäki. *Life cycle costs in heating, ventilation and air conditioning systems with drive*, Master's thesis, Lappeenranta University of Technology, Lappeenranta, March 2008

[15] Siren K. *Simulation and optimization of building energy systems*, Post-graduate seminar on HVAC-technology, Helsinki University of Technology, Helsinki, 2007

[16] Kalle.Riihimäki. *Simulation and optimization model for paper machine hall ventilation system*, Ene-58.152 Postgraduate seminar on HVAC, Helsinki University of Technology, 2007

[17] Kalyanmoy Deb. *MultiObjective Optimization using Evolutionary Algorithms*, John Wiley Sons Ltd, Baffins Lane, Chichester, West Sussex P019 1UD, England , 2001, ISBN: 0-471-87339-X

[18] Kaisa Miettinen and Marko M. Mäkelä and Pekka Neittaanmaki and Jacques Periaux. *Evolutionary Algorithms in Engineering and Computer Science*, John Wiley Sons Ltd, Baffins Lane, Chichester, West Sussex P019 1UD, England, 1999, ISBN: 0-471-99902-4

[19] Jean Dipama and Alberto Teyssedou and Mikhail Sorin. *Synthesis of heat exchanger networks using genetic algorithms*, Applied Thermal Engineering, Vol 28, pages 1763-1773, November 2007

[20] Mitsuo Gen and Runwei Cheng. *Genetic Algorithms Engineering Optimization*, John Wiley Sons,Inc., United States of America , 2000, ISBN: 0-471-31531-1

[21] Kalyanmoy Deb, and Amrit Pratap, and Sameer Agarwal, and T. Meyarivan. *A Fast and Elitist MultiObjective Genetic Algorithm: NSGA-II*, IEEE Transactions on Evolutionary Computation, Vol 6, pages 182-197, April 2002

[22] Rahul B. Kasat and et al. *Multiobjective Optimization of Industrial FCC units using Elitist Nondominated Sorting Genetic Algorithm*, Ind. Eng. Chem. Res, India, Vol 41, pages 4765-4776, 2002

[23] Ruey S. Tsay. *Analysis of Financial Time Series*, Second Edition, John Wiley Sons,Inc., Canada, 2005, ISBN: 0-471-69074-0

[24] Dmitri Kavetski and Stewart W. Franks and George Kuczera. *Confronting Input Uncertainty in Environmental Modelling*, AGU Water Science and Applications Series, Vol 6, pages 49-68, 2002

[25] Antti Solonen. *Monte Carlo methods in parameter estimation of nonlinear models*, Master's thesis, Lappeenranta University of Technology, Lappeenranta, December 2006

[26] Peter Congdon. *Bayesian Statistical Modelling*, Second Edition, John Wiley Sons Ltd, England , 2006, ISBN: 0-470-01875-5

[27] Heikki Haario. *Statistical Analysis in Modelling: MCMC Methods*, Lecture Material, Lappeenranta University of Technology, Lappeenranta, 2007

[28] Gilks, W., S. Spiegelhalter D. *Markov Chain Monte Carlo in Practice*, New York, USA: Springer Science + Business Media, ISBN:0-412-05551-1

[29] Lieke Wang and Bengt Sunden. *Optimal design of plate heat exchanger with and without pressure drop specifications*, Applied Thermal Engineering, Vol 23, pages 295-311, 2003

Appendix I. Newton's Law of Cooling

The mean temperature T_m is a convenient reference temperature for internal flows, playing much the same role as the free stream temperature T_∞ for external flows which is constant in the flow direction. Accordingly, Newton's law of cooling may be expressed as

$$\Phi = \alpha(T_s - T_m)$$

where α is the *local* convection heat transfer coefficient, T_s is the temperature at the surface, and T_m is the mean temperature which is varying in the flow direction [1].

Appendix II. Derivation of log mean temperature difference ($\triangle T_{lm}$)

Applying an energy balance to each of the differential elements of Figure 6, it follows that

$$d\Phi = -q_{m,h}c_{p,h}dT_h \equiv -C_h dT_h$$

and

$$d\Phi = q_{m,c}c_{p,c}dT_c \equiv C_c dT_c$$

where c_h and c_c are the hot and cold fluid *heat capacity rates*, respectively. These expressions may be integrated acros the heat exchanger to obtain the overall energy balances given by Equations 8 and 9. The heat transfer across the surface area dA may also be expressed as

$$d\Phi = U\Delta T dA$$

where $\Delta T = T_h - T_c$ is the *local* temperature difference between the hot and cold fluids.

To determine the integrated form of Equation 14, we begin by substituting Equations 12 and 13 into the differential form of Equation 10.

$$d(\Delta T) = dT_h - dT_c$$

to obtain

$$d(\Delta T) = -d\Phi\left(\frac{1}{C_h} + \frac{1}{C_c}\right)$$

Substituting for $d\Phi$ from the previous equation and integrating acros the heat exchanger, we obtain

$$\int_1^2 \frac{d(\Delta T)}{\Delta T} = -U\left(\frac{1}{C_h} + \frac{1}{C_c}\right)\int_1^2 dA$$

or

$$\ln\left(\frac{\Delta T_2}{\Delta T_1}\right) = -UA\left(\frac{1}{C_h} + \frac{1}{C_c}\right)$$

Substituting for C_h and C_c from Eqautions 3 and 4, respectively, it follows that

$$\begin{aligned}\ln\left(\frac{\Delta T_2}{\Delta T_1}\right) &= -UA\left(\frac{T_{h,i}-T_{h,o}}{\Phi}+\frac{T_{c,o}-T_{c,i}}{\Phi}\right)\\ &= -\frac{UA}{\Phi}[(T_{h,i}-T_{c,i})-(T_{h,o}-T_{c,o})]\end{aligned}$$

Recognazing that, for the parallel-flow heat exchanger, $\Delta T_1 = (T_{h,i} - T_{c,i})$ and $\Delta T_2 = (T_{h,o} - T_{c,o})$,we then obtain

$$\Phi = UA\frac{\Delta T_2 - \Delta T_1}{\ln(\Delta T_2/\Delta T_1)}$$

Comparing the above expression with Equation 11, we conclude that the appropriate average temperature difference is a *log mean temperature difference*, ΔT_{lm}. Accordingly, we may write

$$\Phi = UA\Delta T_{lm}$$

where

$$\Delta T_{lm} = \frac{\Delta T_2 - \Delta T_1}{\ln(\Delta T_2/\Delta T_1)} = \frac{\Delta T_1 - \Delta T_2}{\ln(\Delta T_1/\Delta T_2)}$$

Remember that, for the *parallel-flow exchanger*,

$$\begin{cases}\Delta T_1 &= T_{h,1} - T_{c,1} = T_{h,i} - T_{c,i}\\ \Delta T_2 &= T_{h,2} - T_{c,2} = T_{h,o} - T_{c,o})\end{cases}$$

Appendix III. Effectiveness of dry heat exchanger-NTU methods

For any heat exchanger, the effectiveness can be expressed as

$$\epsilon = f\left(NTU, \frac{C_{min}}{C_{max}}\right)$$

where

$$\frac{C_{min}}{C_{max}} = \frac{C_c}{C_h} = \frac{C_h}{C_c}$$

depending on the relative magnitude of the hot and cold fluid heat capacity rates, and

$$NTU = \frac{UA}{C_{min}}$$

Appendix IV. Crowding Distance

The crowding distance is a measure of how close an individual is to its neighbors. Large average crowding distance will result in better diversity in the population. The crowding distance is calculated as follows:
For each front F_i, n is the number of individuals.

1. initialize the distan.ce to be zero for all the individuals i.e. $F_i(d_j) = 0$, where j corresponds to the j^{th} individual in front F_i

2. for each objective function m

   - Sort the individuals in front F_i based on objective m i.e. $I = sort(F_i, m)$.

   - Assign infinite distance to boundary values for each individual in F_i i.e. $I(d_1) = \infty$ and $I(d_n) = \infty$

   - for $k = 2$ to $n - 1$
     - $I(d_k) = I(d_k) + \frac{I(k+1)m - I(k-1)m}{f_m^{max} - f_m^{min}}$

     - $I(k)m$ is the value of the m^{th} objective function of the k^{th} individual in I.

The basic idea behind the crowding distance is finding the euclidian distance between each individual in a front based on their m objectives in the m dimensional hyper space. The individuals in the boundary are always selected since they have infinite distance assignment.

Appendix V. Economic factors calculation

Economic factors should be taken into account during the analysis of any investment profitability. As the inflation rate and interest rate vary with time, the investment and operating costs should be discounted to the present value of money. In this project, the economic factors are calculated as follows:

$$r = \frac{i - f}{1 + f}$$

$$r_e = \frac{r - a_e''}{1 + a_e''}$$

$$r_h = \frac{r - a_h''}{1 + a_h''}$$

$$d_e = \frac{1 - (1 + r_e)^{1/t}}{r_e}$$

$$d_h = \frac{1 - (1 + r_h)^{1/t}}{r_h}$$

$$a' = \frac{1 - (1 + r)^{1/t}}{r}$$

where

t	life time span of the project
i	nominal interest rate
f	inflation rate
r	real interest rate
$a_e^{''}$	escalation term for electrical energy
$a_h^{''}$	escalation term for heat energy
r_e	real interest rate for electrical energy
r_h	real interest rate for heat energy
d_e	discount term for electrical energy
d_h	discount term for heat energy
$a^{'}$	discount term for inflation or present value